Coherent synchrotron radiation instability in low-emittance electron storage rings

Demin Zhou

Accelerator theory group, Accelerator laboratory, KEK

Acknowledgements

T. Agoh, K. Bane, M. Blaskiewicz, A. Blednykh, Y. Cai, Y.-C Chae, S. Dastan, R. Lindberg, S. Di Mitri, E. Karantzoulis, S. Kramer, K. Ohmi, K. Oide, G. Stupakov, N. Yamamoto, K. Yokoya

ビーム物理研究会・若手の会2023, 東北大学電子光理学研究センター, 仙台, Mar. 4, 2024

Outline

- Motivation
- Introduction to coherent synchrotron radiation
- CSR impedance calculation using CSRZ code
- Theories of CSR driven microwave instability (MWI) threshold
- Prediction of CSR instability via simulations
    - Interplay of CSR, CWR, RW and geometric wakes
- Summary

Motivation

- 2009-: Coherent Synchrotron Radiation (CSR) in (KEKB and) SuperKEKB
  - CSR appears in J-ARC, damping ring (DR), beam transport (BT) lines and arcs of main rings.
- 2011-: CSR as THz light sources (wanted) and as source of microbunching instability (unwanted).
  - Through CSR, I many found collaborators outside collider community.

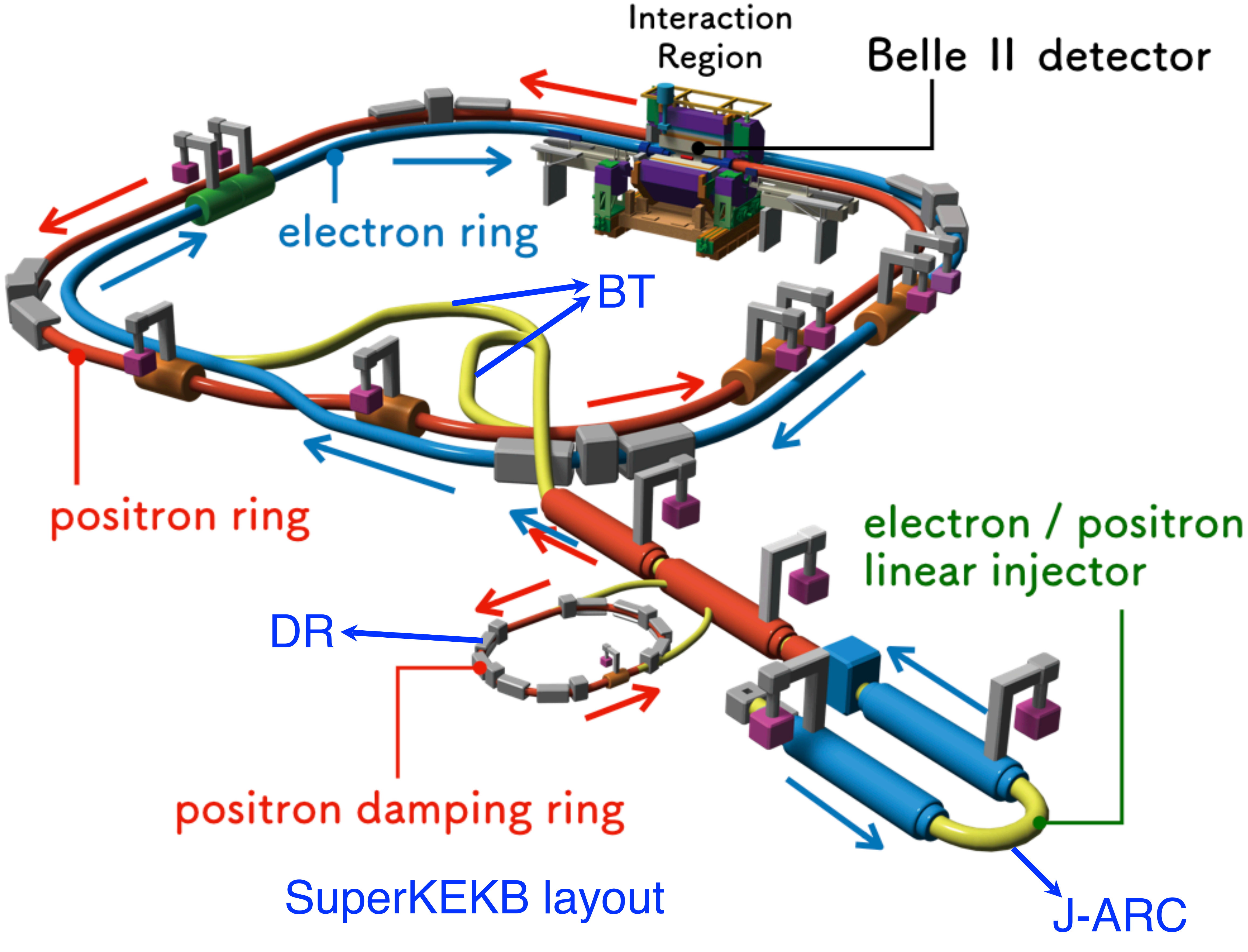

SuperKEKB layout

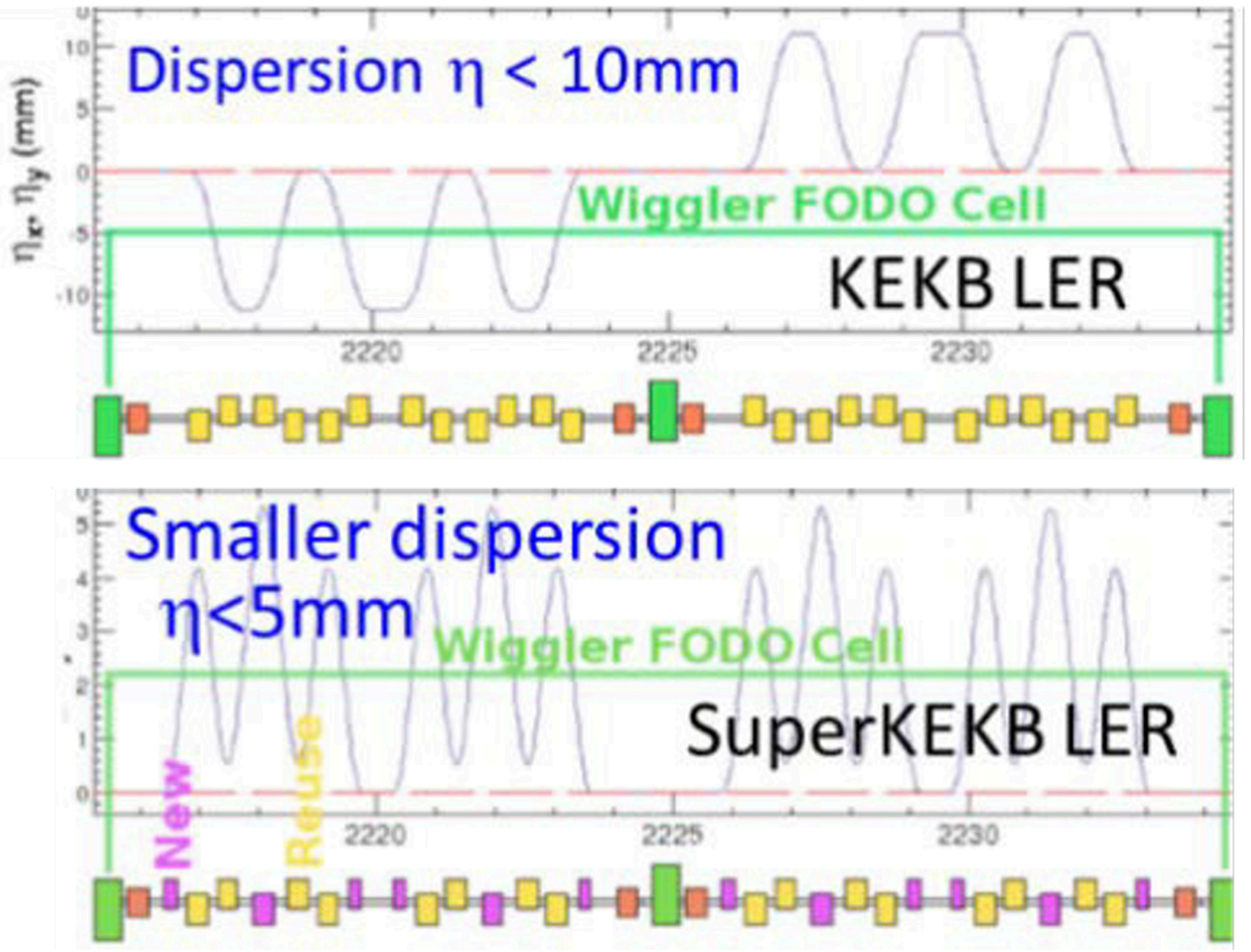

Wigglers in SuperKEKB LER [2]

Wigglers:
$\rho \approx$ 15 m (Minimum value), $\lambda_w \approx$ 1.1 m
Total length of wiggler sections ~300 m

Dipoles: $h = 45$ mm, $\rho = 74.7$ m

[1] T. Ishibashi et al 2024 JINST 19 P02013. [2] T. Miura et al., IPAC2015, TUYB1.

Introduction to coherent synchrotron radiation

- CSR has been a hot topic of accelerator physics: Theories, simulations and measurements of CSR fields and CSR-driven beam instabilities in electron storage rings and FELs; design of linac- and ring-based CSR THz sources.

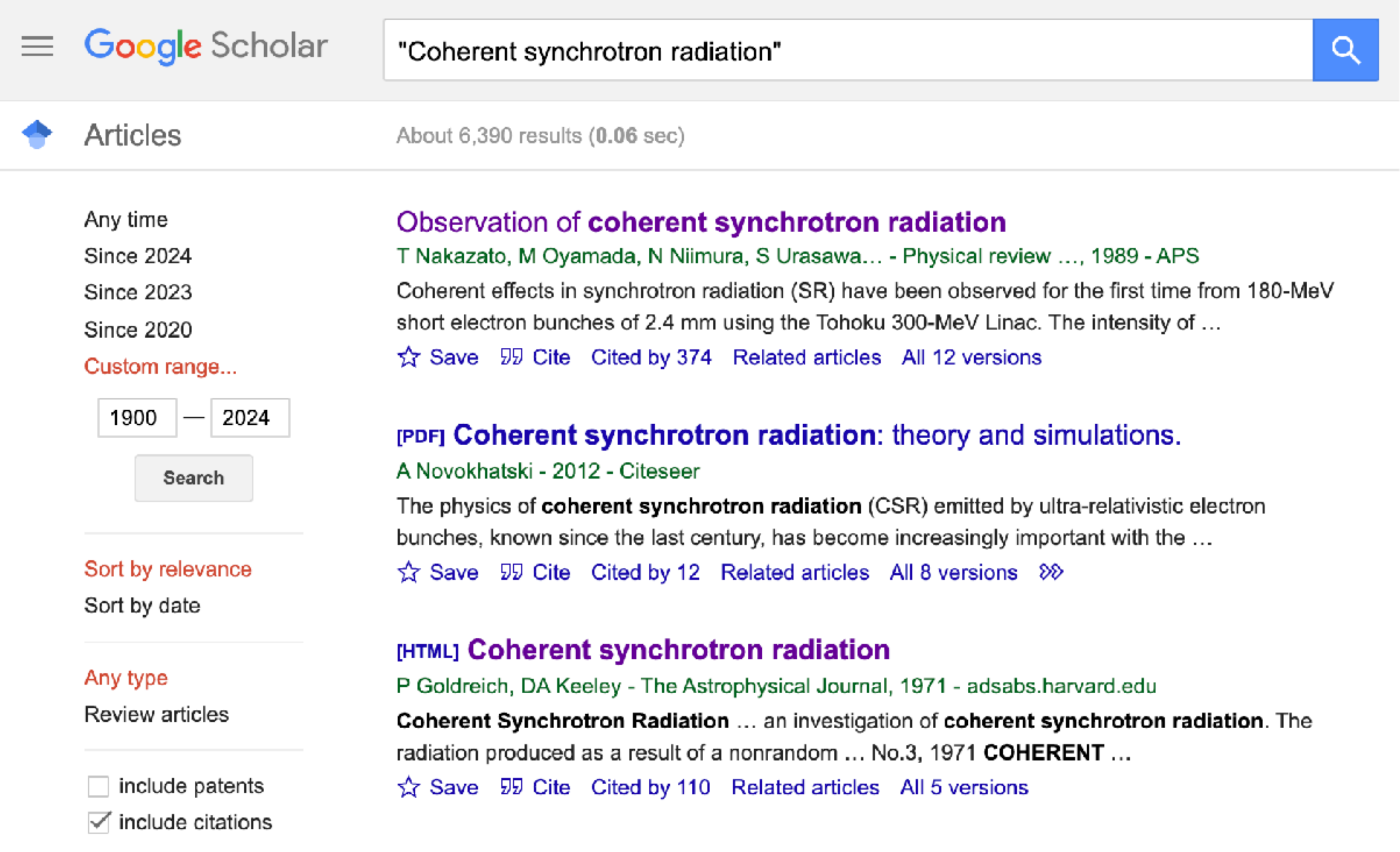
Google Scholar
"Coherent synchrotron radiation"
Articles
About 6,390 results (0.06 sec)
Any time
Since 2024
Since 2023
Since 2020
Custom range...
1900 — 2024
Search
Sort by relevance
Sort by date
Any type
Review articles
include patents
include citations

Observation of coherent synchrotron radiation
T Nakazato, M Oyamada, N Niimura, S Urasawa… - Physical review …, 1989 - APS
Coherent effects in synchrotron radiation (SR) have been observed for the first time from 180-MeV short electron bunches of 2.4 mm using the Tohoku 300-MeV Linac. The intensity of …
Save Cite Cited by 374 Related articles All 12 versions

[PDF] Coherent synchrotron radiation: theory and simulations.
A Novokhatski - 2012 - Citeseer
The physics of coherent synchrotron radiation (CSR) emitted by ultra-relativistic electron bunches, known since the last century, has become increasingly important with the …
Save Cite Cited by 12 Related articles All 8 versions

[HTML] Coherent synchrotron radiation
P Goldreich, DA Keeley - The Astrophysical Journal, 1971 - adsabs.harvard.edu
Coherent Synchrotron Radiation … an investigation of coherent synchrotron radiation. The radiation produced as a result of a nonrandom … No.3, 1971 COHERENT …
Save Cite Cited by 110 Related articles All 5 versions


Google Scholar
"コヒーレント放射光"
Articles
About 153 results (0.07 sec)
Any time
Since 2024
Since 2023
Since 2020
Custom range...
1900 — 2024
Search
Sort by relevance
Sort by date
Any type
Review articles
include patents
include citations

Tip: Search for English results only. You can specify your search language in Scholar Settings.

コヒーレント放射光
高橋俊晴 - 加速器, 2005 - jstage.jst.go.jp
Since coherent synchrotron radiation (CSR) from short bunches of electrons was first observed in 1989, several types of coherent radiation have been studied experimentally using …
Save Cite Cited by 3 Related articles

コヒーレント放射光
池沢幹彦 - 日本物理学会誌, 1990 - jstage.jst.go.jp
総数 AW からなる高エネルギー電子の集団 (バンチ) が放射光を発するとき,「通常」 の放射光の強度は AV に比例する. 一方, 長波長領域で放射光の波長がバンチの進行方向の長さより遥かに大きく…
Save Cite Cited by 2 Related articles All 5 versions

コヒーレント放射光の応用
池沢幹彦 - 日本物理学会誌, 1998 - jstage.jst.go.jp
… 現在,東 北大核理研にも**コヒーレント放射光**を光源とした分光装置 が設置されつつある.更に次世代の光源となり得るのはマ イクロバンチFELである.速やかに開発して実用化しなけ ればならない….
Save Cite Cited by 3 Related articles All 5 versions

→

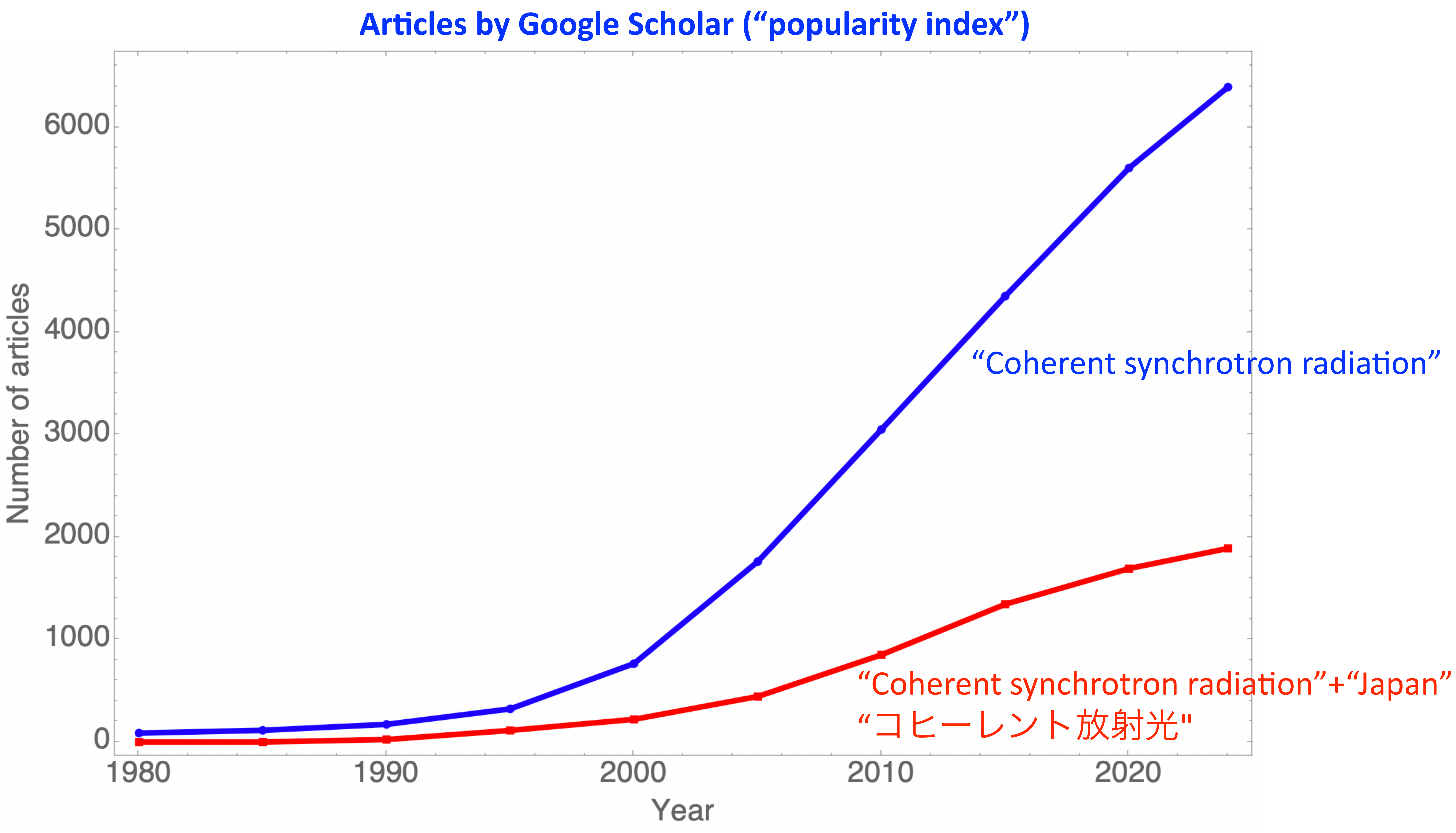

Introduction to coherent synchrotron radiation (cont'd)

- Radiation of moving charges with acceleration $\dot{\vec{\beta}} \neq 0$ expressed by Lienard-Wiechert fields [1]:

$$\vec{E}(\vec{r},t) = \frac{e}{4\pi\epsilon_0}\left[\frac{\vec{n}-\vec{\beta}}{\gamma^2(1-\vec{\beta}\cdot\vec{n})^3R^2}\right]_{\text{ret}} + \frac{e}{4\pi\epsilon_0 c}\left[\frac{\vec{n}\times\{(\vec{n}-\vec{\beta})\times\dot{\vec{\beta}}\}}{(1-\vec{\beta}\cdot\vec{n})^3R}\right]_{\text{ret}}$$

- Synchrotron radiation
  - Observed in particle accelerators [4], and popularly used as light sources [5].

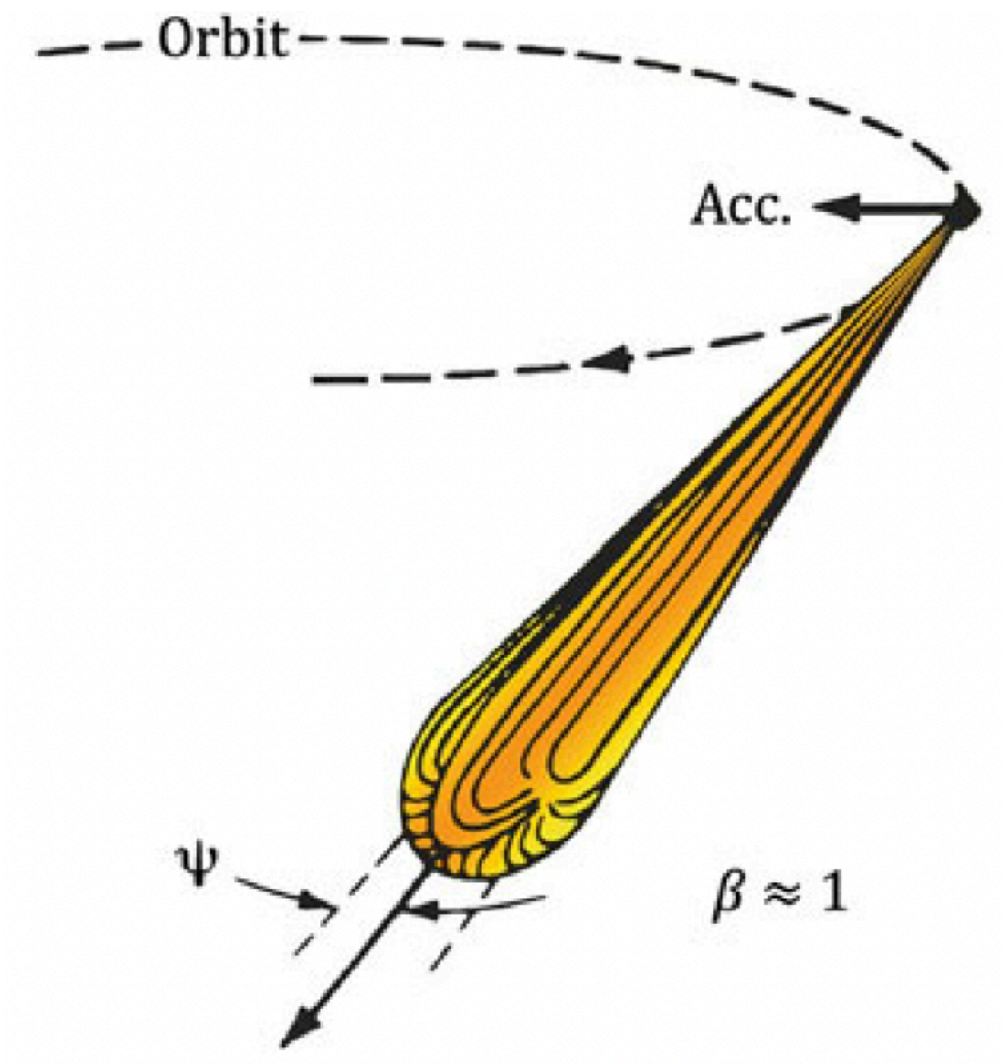

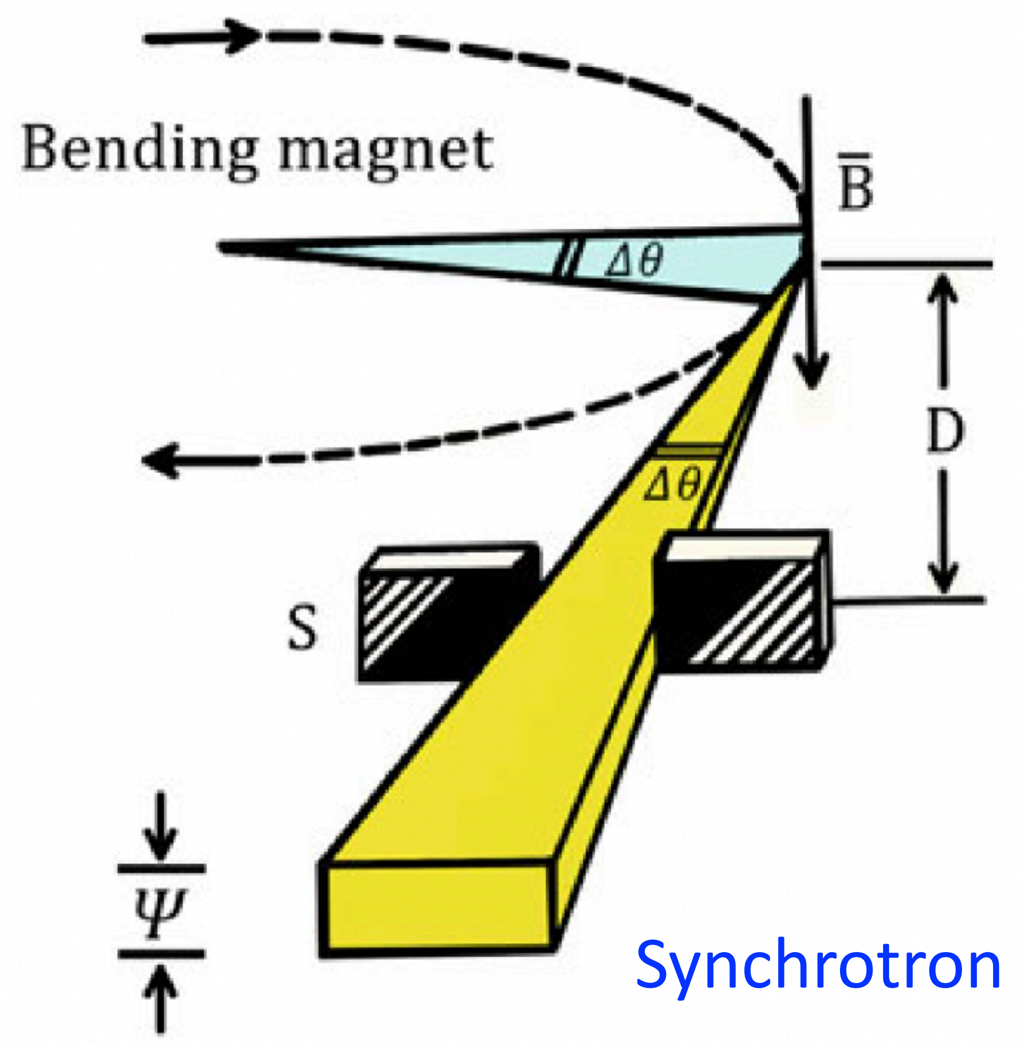

Synchrotron radiation [5]

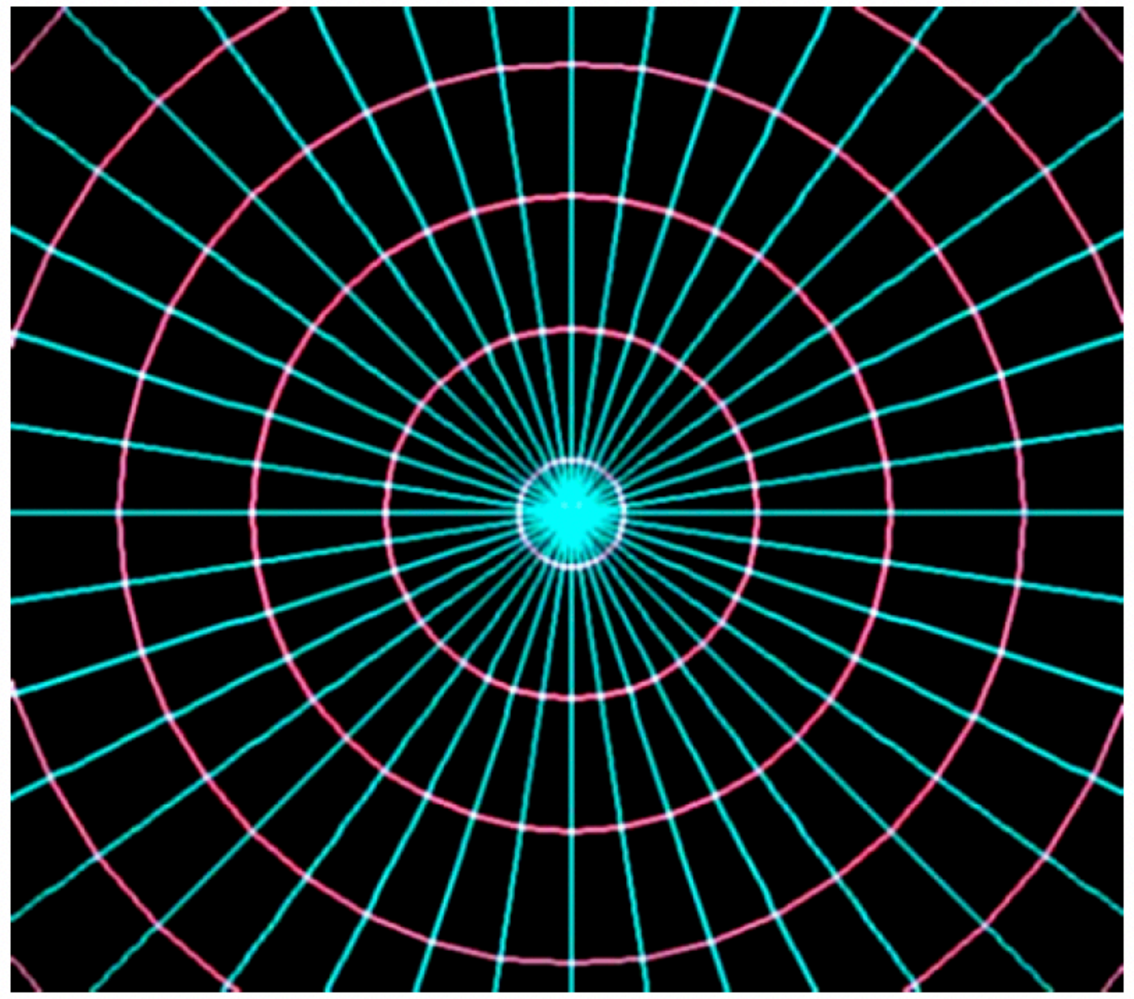

Fig. 3 Static field. Snapshot from the Radiation 2D.

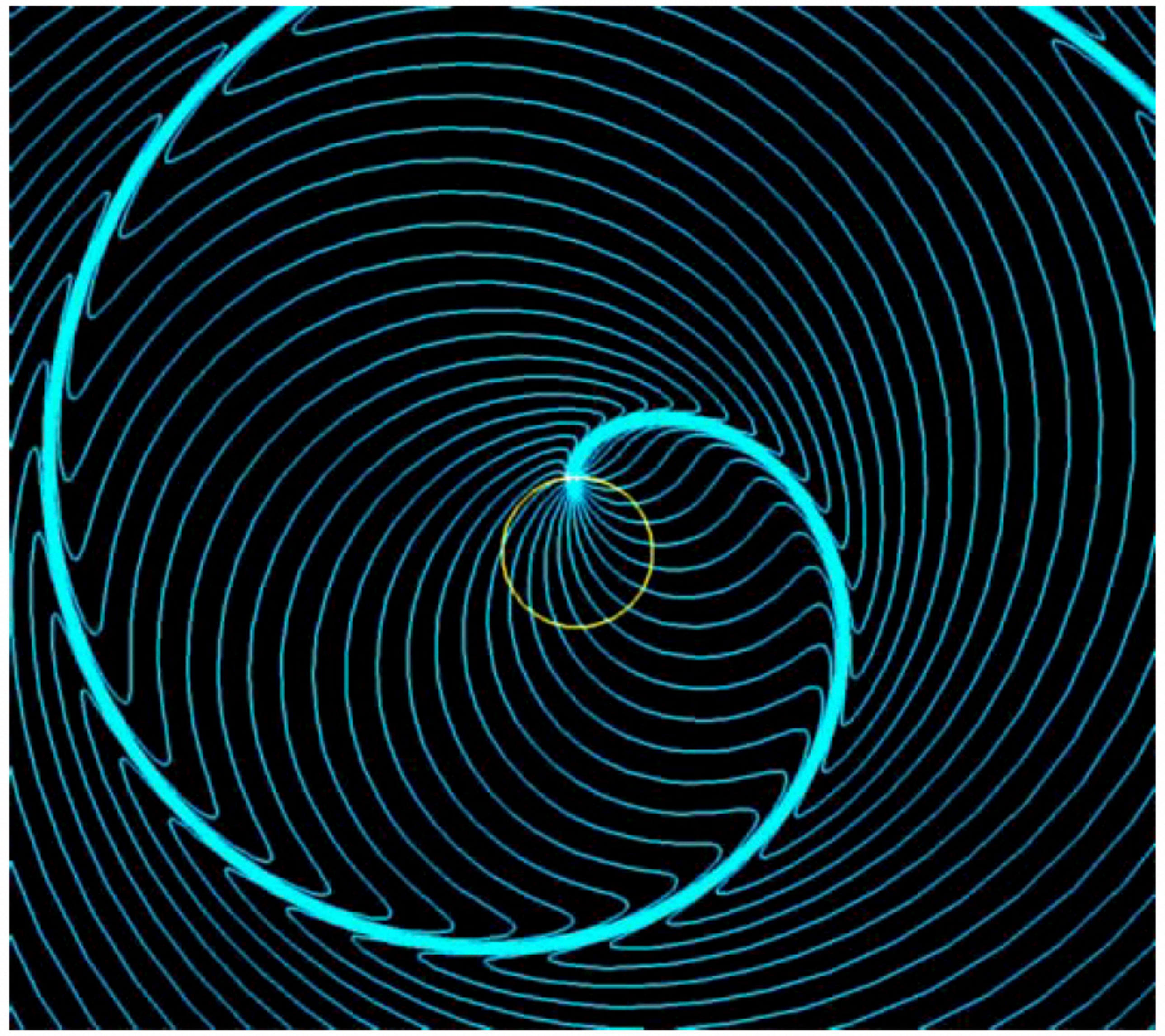

Fig. 4 Synchrotron radiation at v = 0.9c. Snapshot from the Radiation 2D.

Visualization of synchrotron radiation [2,3]

[1] J.D. Jackson, Classical Electrodynamics (2021). [2] T. Shintake, LINAC2002, TH426. [3] https://groups.oist.jp/qwmu/software.
[4] F.R. Elder et al., Phys. Rev. 71, 829 (1947). [5] S. Mobilio et al., Synchrotron Radiation (2016).

Introduction to coherent synchrotron radiation (cont'd)

- Coherent synchrotron radiation (CSR)
  - CSR in particle accelerators was first recognized by J. Schwinger [1]
  - First measured by T. Nakazato et al. in linac at Tohoku Univ. [2]
  - First measured in storage ring at MAX-I [3]
  - A nice historical review by T. Takahashi [4]
- Fundamental features of CSR
  - Coherent radiation ($U \propto N^2$) at wavelengths $\lambda > \sigma_z$ or due to microbunching

$$\left.\frac{dU}{dk}\right|_{bunch} = \left[N + N(N-1)\left|\tilde{\lambda}(k)\right|^2\right]\frac{dU}{dk}$$

Free-space steady-state:

$$\frac{dU}{dk} = \frac{e^2}{4\pi\epsilon_0}\sqrt{3}\gamma\frac{k}{k_C}\int_{k/k_C}^{\infty} K_{5/3}(x)dx$$

Gaussian bunch:

$$\tilde{\lambda}(k) = e^{-k^2\sigma_z^2/2}$$

  - dU/dk is complicated with wall shielding and transients
  - Coherent radiation is useful to generate THz lights
  - Coherent radiation is detrimental for 4th generation ring- or linac-based light sources

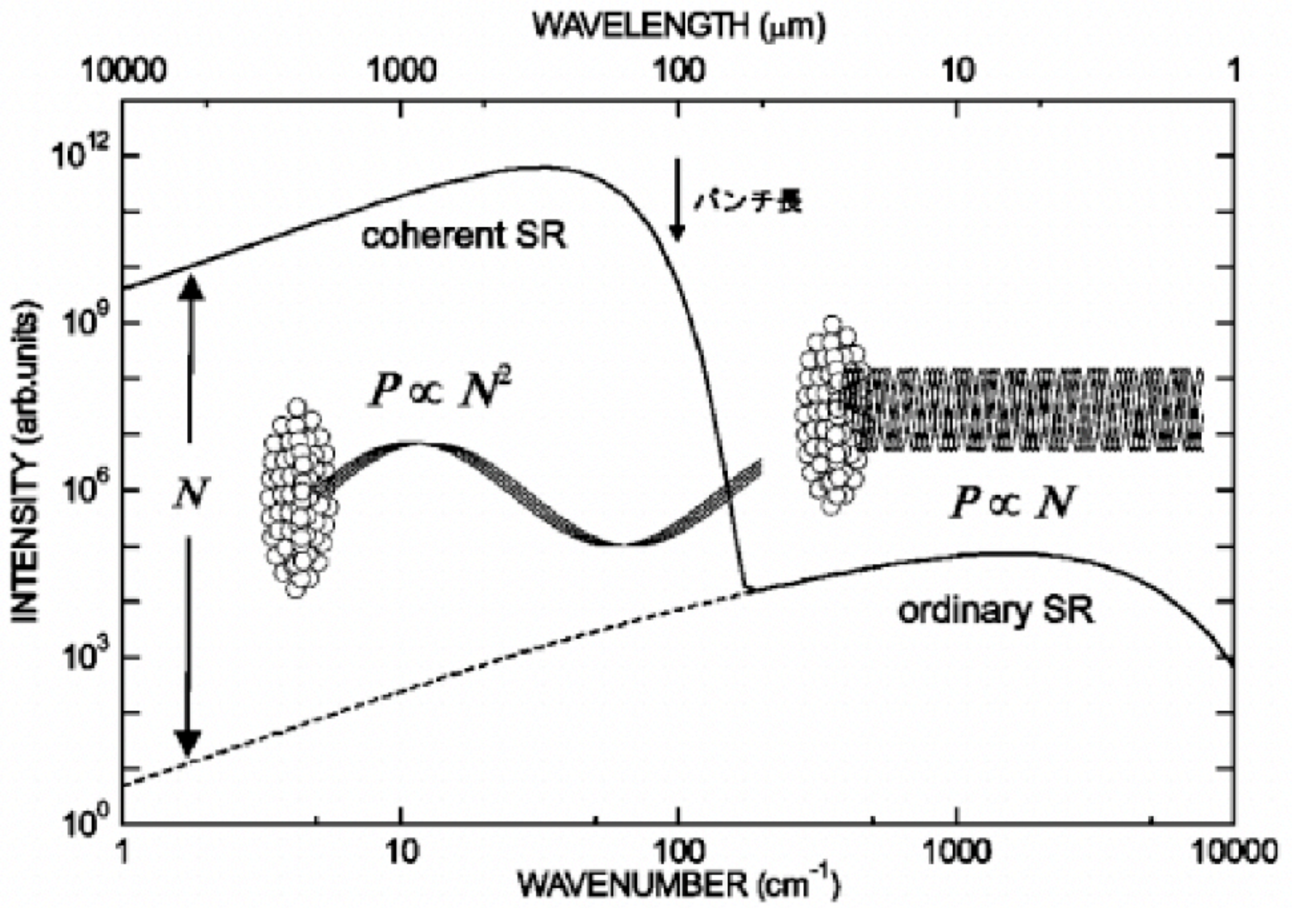

図 1　コヒーレント放射光の模式図．通常，放射光強度はバンチ内電子数 N に比例するが，バンチ長よりも長波長側では位相が揃って重なり合いコヒーレント放射光となり，N の 2 乗に比例する．なお，スペクトルの計算では Gaussian バンチ（FWHM 0.1 mm）を仮定している．

Coherent synchrotron radiation [4]

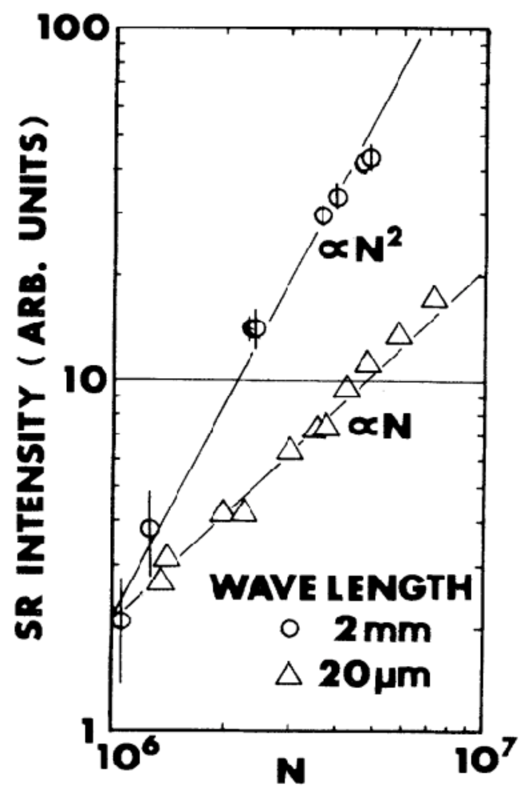

FIG. 3. Beam-current dependence of the SR intensity. N is the number of electrons in a bunch, which is proportional to the electron beam current. The SR intensity is proportional to N^2 at a wavelength of 2 mm, while to N at 20 μm. The values of intensity should not be compared between the two wavelengths.

First observation of CSR [2]

[1] J. Schwinger, Phys. Rev. 70, p. 798 (1946). [2] T. Nakazato et al., Phys. Rev. Lett. 63, 1245 (1989).
[3] A. Andersson et al. "Observation of coherent synchrotron radiation from a 1-mm electron bunch at the MAX-I storage ring", 1999. [4] 高橋 俊晴, コヒーレント放射光, 「加速器」Vol. 2, No.1, 2005.

Introduction to coherent synchrotron radiation (cont'd)

- Fundamental features of CSR
  - Most subtleties of CSR lie in the "overtaking" fields
  - Standard theories of wakefields [2] do not apply to CSR
    - Panofsky-Wenzel theorem
    - Causality and resulting Hilbert-transform relation of impedance

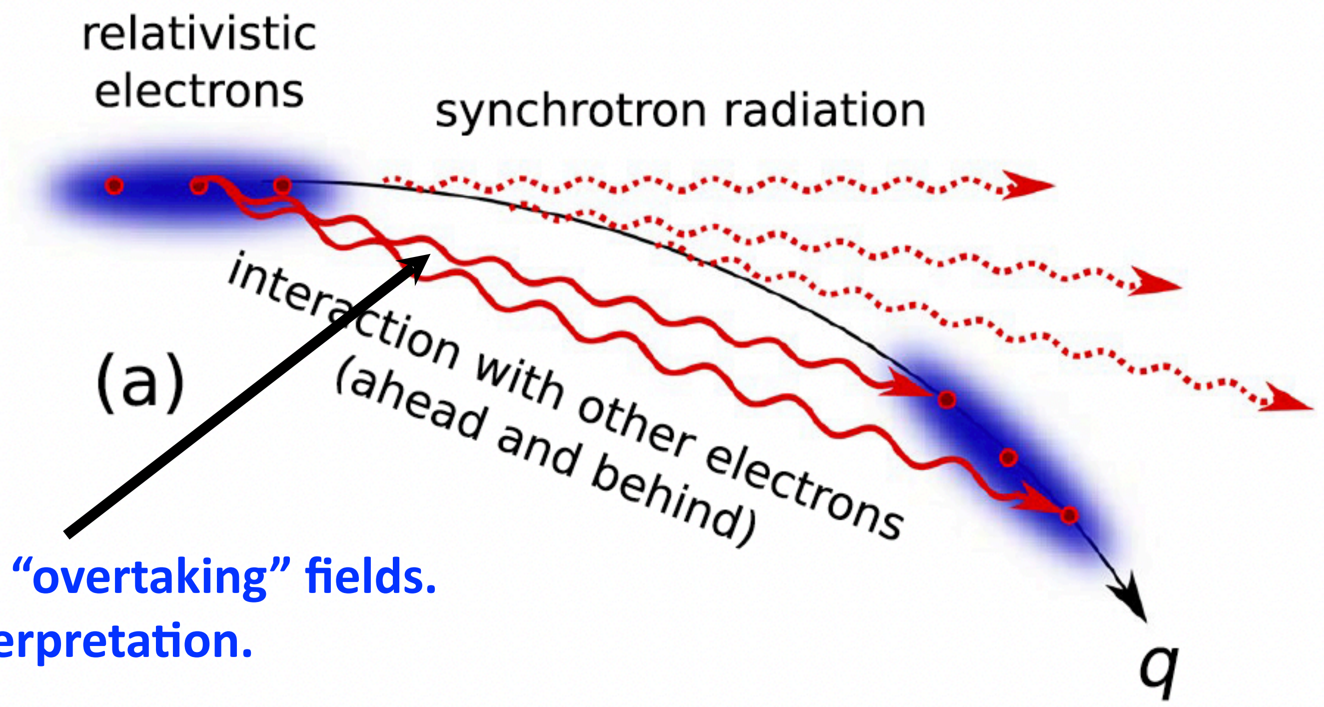

Comment:
"Lienard-Wiechert" viewpoint of "overtaking" fields.
Personally, I do not favor this interpretation.

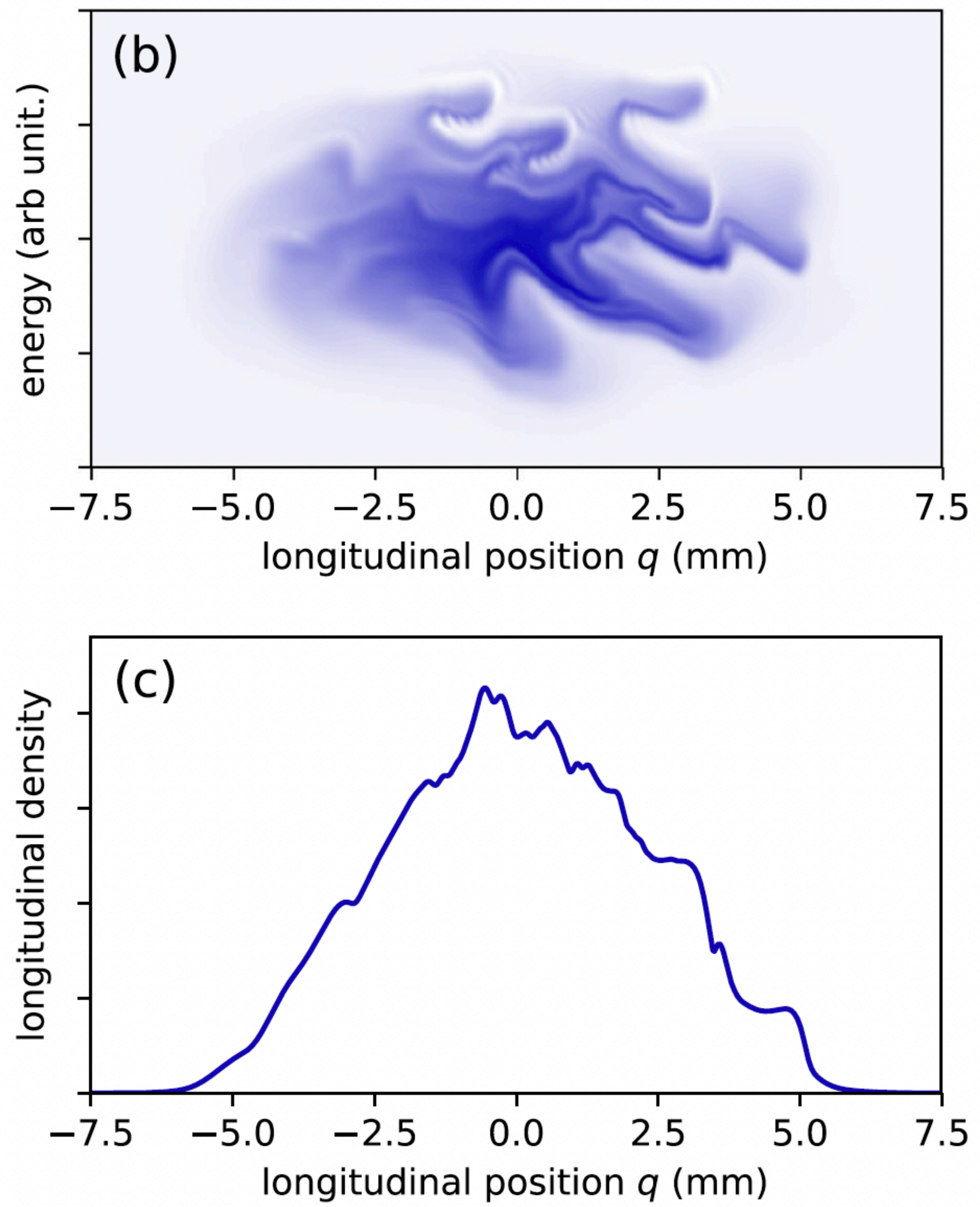

Microbunching driven by CSR [1]

Definition of wake function:

$$\tau = d/v = (z_0 - z)/v \qquad \overline{\vec{F}}(\vec{r},\vec{r}_0;\tau) = \int_{-\infty}^{\infty} dt\ v\ \vec{F}(\vec{R},\vec{R}_0;t)\Big|_{z_0=vt,z=vt-d}.$$

$$w_z(\vec{r},\vec{r}_0;d) = -\frac{1}{q_0q_1}\overline{F}_z(\vec{r},\vec{r}_0;\tau), \qquad w_\perp(\vec{r},\vec{r}_0;d) = \frac{1}{q_0q_1}\overline{F}_\perp(\vec{r},\vec{r}_0;\tau),$$

Fourier-transform pair of wake function and impedance:

$$w_z(\vec{r},\vec{r}_0;d) = \frac{1}{2\pi}\int_{-\infty}^{\infty} d\omega\ Z_\parallel(\vec{r},\vec{r}_0;\omega)e^{-i\omega\tau}, \qquad w_\perp(\vec{r},\vec{r}_0;d) = \frac{1}{2\pi\kappa}\int_{-\infty}^{\infty} d\omega\ Z_\perp(\vec{r},\vec{r}_0;\omega)e^{-i\omega\tau}.$$

Hilbert-transform relation of impedance:

$$\mathrm{Re}\{Z(\omega)\} = \frac{2}{\pi}\mathrm{P.V.}\int_0^\infty \frac{\omega'\mathrm{Im}\{Z(\omega')\}}{\omega'^2-\omega^2}d\omega', \qquad \mathrm{Im}\{Z(\omega)\} = -\frac{2\omega}{\pi}\mathrm{P.V.}\int_0^\infty \frac{\mathrm{Re}\{Z(\omega')\}}{\omega'^2-\omega^2}d\omega'.$$

[1] S. Bielawski et al., Scientific reports 9.1 (2019): 10391. [2] A. Chao, "Physics of collective beam instabilities in high energy accelerators", 1993.

CSR impedance calculation

- Impedance calculation based on parabolic equation
  - G. Stupakov, T. Agoh et al. developed the method of calculating CSR impedance using parabolic equation (PE).
  - My CSRZ ("Z" means impedance) code follows this line to solve PE [1]:

$$\frac{\partial \vec{E}_\perp}{\partial s} = \frac{i}{2k}\left[\nabla_\perp^2 \vec{E}_\perp - \frac{1}{\epsilon_0}\nabla_\perp \rho_0 + 2k^2\left(\frac{x}{R(s)} - \frac{1}{2\gamma^2}\right)\vec{E}_\perp\right]$$

$$E_s = \frac{i}{k}\left(\nabla_\perp \cdot \vec{E}_\perp - \mu_0 c J_s\right) \qquad Z(k) = -\frac{1}{q}\int_0^\infty E_s(x_c, y_c)ds$$

Note:

$$\mathrm{Re}[Z_\parallel(k)] = \frac{\pi}{e^2 c}\frac{dU(k)}{dk}$$

  - CSRZ takes into account: Arbitrary curvature of beam orbit $R(s)$ (CSR), finite beam energy γ (space charge effects, SC), and resistive wall (RW). The total impedance is not a simple sum of $Z_{CSR} + Z_{SC} + Z_{RW}$, but includes their interference.
  - CSRZ uses Gaussian charge distribution in x-y plane, assuming $\sigma_x > \sigma_y$. Self-field is calculated by Bassetti-Erskine formulae.
  - Currently, CSRZ assumes uniform rectangular chamber referring to the beam orbit.
  - See [1] for an overview and [2] for details of CSRZ code.
  - See [3,4,5] for recent applications of CSRZ code.

A single bend

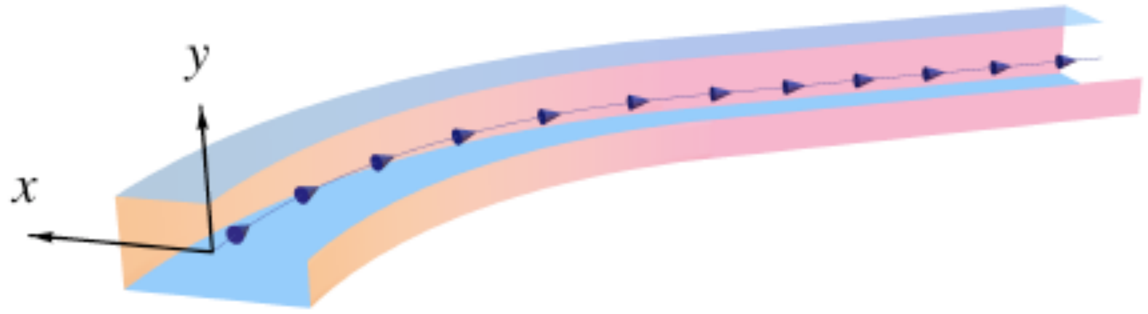

A wiggler with "wiggling" chamber

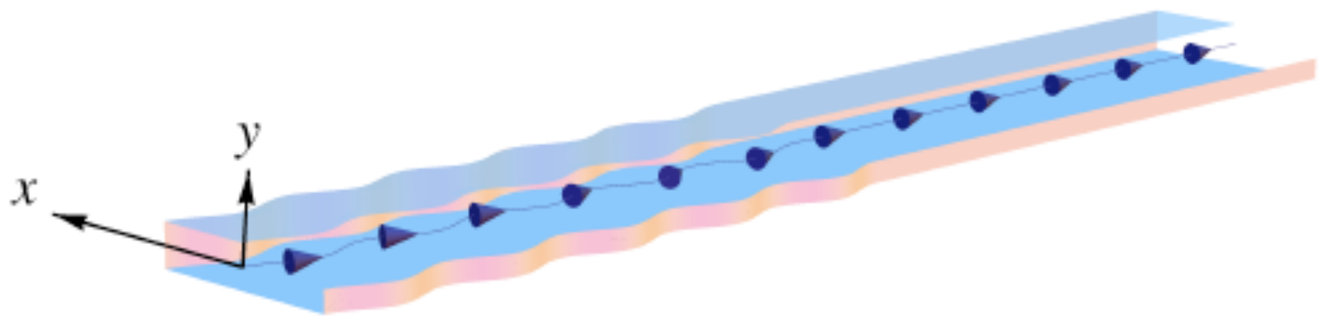

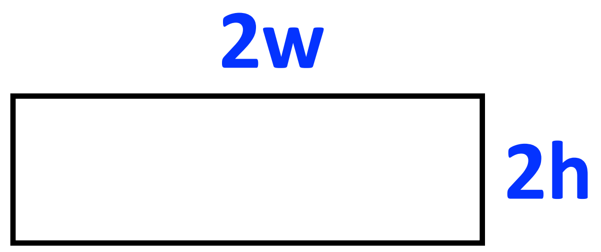

[1] D. Zhou et al., "An Alternative 1D Model for CSR with Chamber Shielding", in Proceedings of IPAC'12, New Orleans, Louisiana, USA.
[2] D. Zhou, Coherent Synchrotron Radiation and Microwave Instability in Electron Storage Rings, Ph.D. thesis, SOKENDAI and KEK, 2011.
[3] G. Stupakov and D. Zhou, PRAB 19, 044402 (2016). [4] A. Gamelin, et al., NIM-A 999 (2021): 165191. [5] L. Carver et al., PRAB 26, 044402 (2023).

CSR impedance calculation (cont'd)

- Examples of CSR impedance by CSRZ
  - A single bend with varied length: w/h=30/15 mm, R=5 m, L_{bend}=0.5/2/8 m.
  - Black/Blue/Red/Green lines: Steady-state parallel-plates/L=0.5/L=2/L=8 m. For convenience of comparison, the impedance amplitude is scaled to L=1 m.
  - "Short bend": Transient effect at the entrance and exit is important.
  - "Long bend": Excited eigenmodes of a toroidal chamber (or "whispering gallery modes" by R. Warnock [1]).
  - "Overtaking field": Short-range wake fields, space charge like.
  - "Trailing field": Long-range wake fields, relevant to excited eigenmodes.

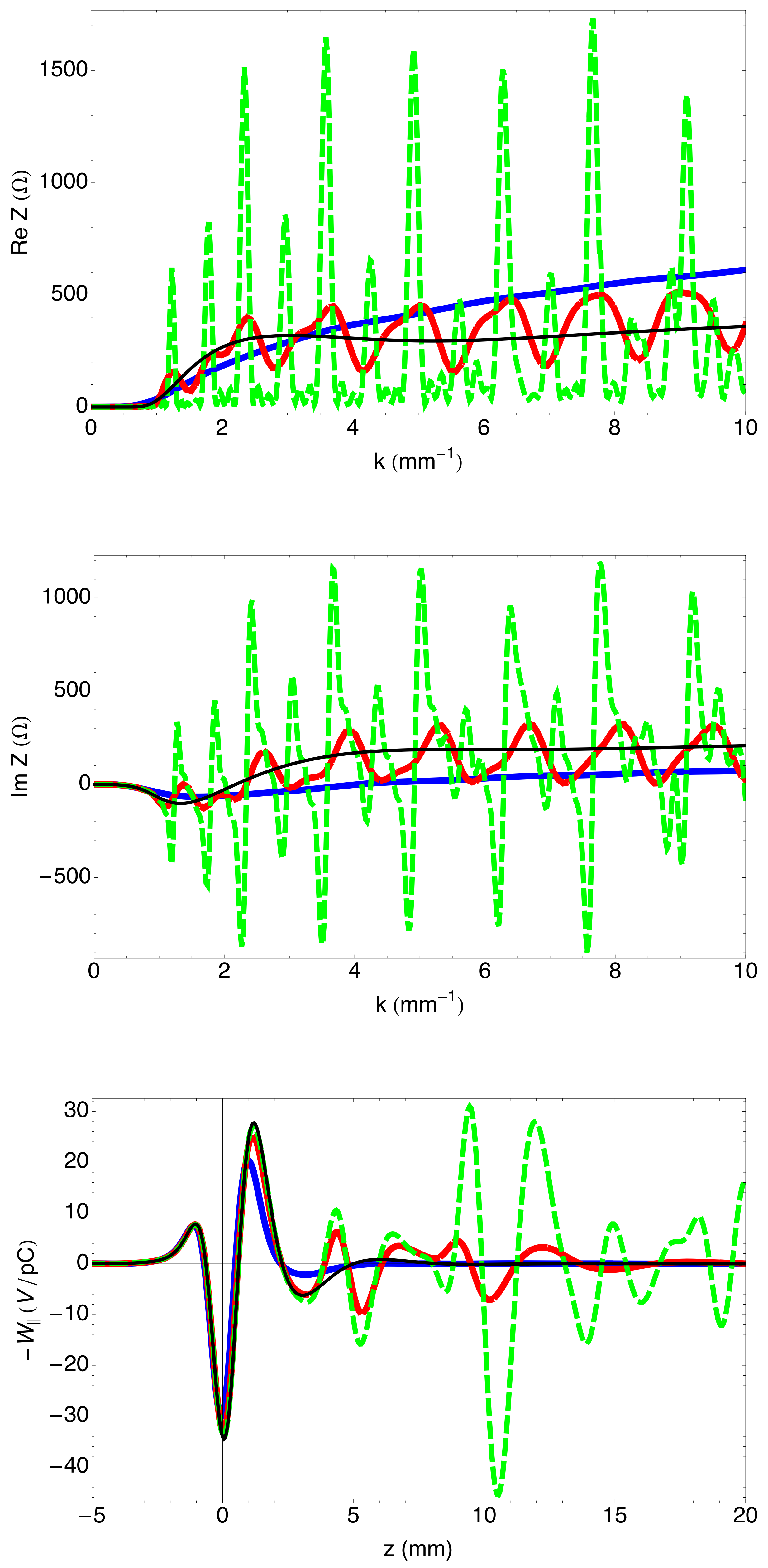

[1] R. Warnock, arXiv:1708.05500.

CSR impedance calculation (cont'd)

- Examples of CSR impedance by CSRZ
  - A realistic ring with multiple-bends: assuming smooth chamber.
  - SuperKEKB DR as an example [1, 2, 3]: a/b=34/34 mm, L_{bend}=0.74/0.29 m, R=2.7/-3 m (reverse bends), L_{drift}=0.9 m, N_{cell}=1/6/16.
  - Multi-bend interference: CSR fields generated by multiple bends propagate along the chamber together with the beam. The fields interfere to produce a pattern of "narrow-band spikes".
  - The real part of CSR impedance should correspond to SR spectrum in measurement.

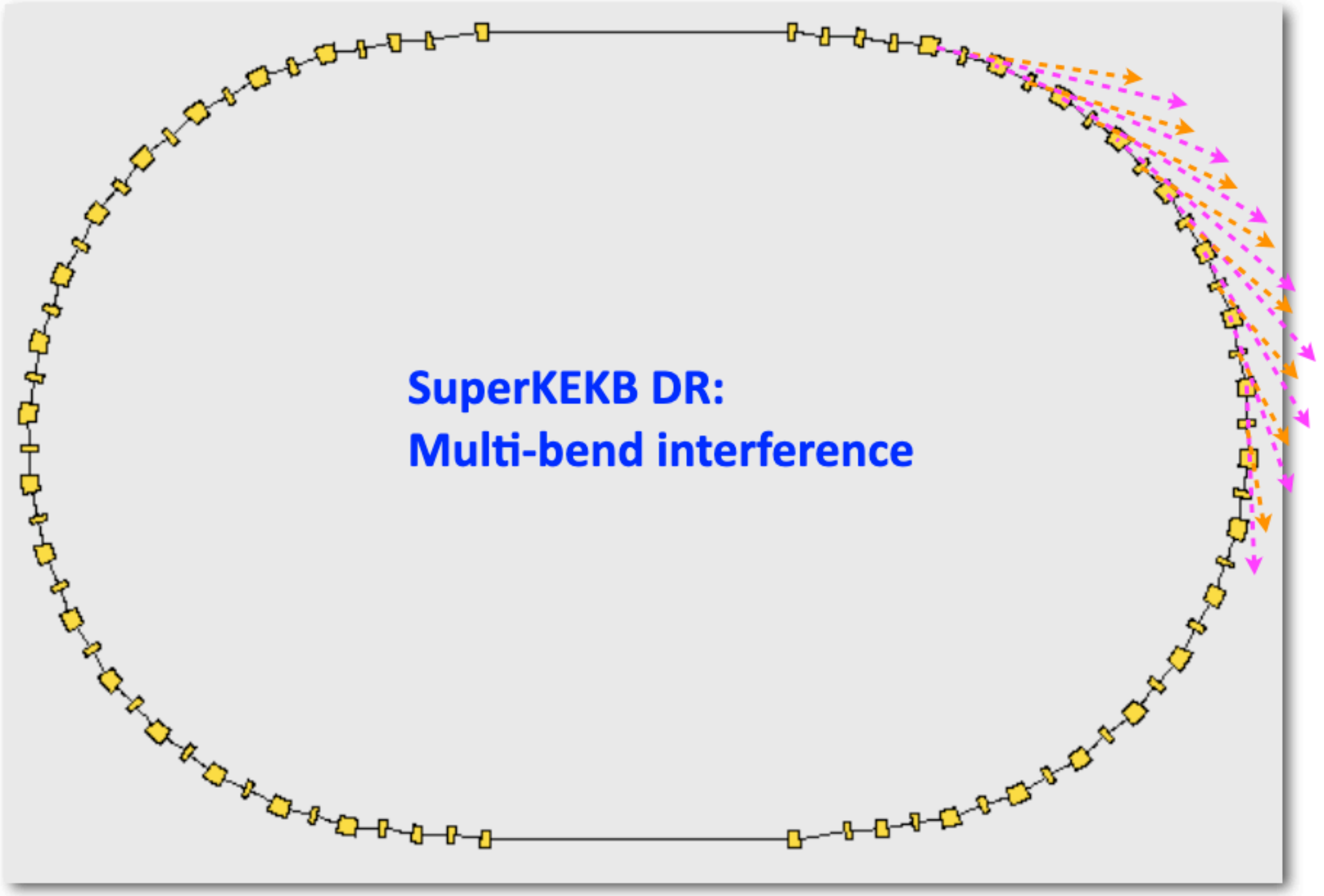

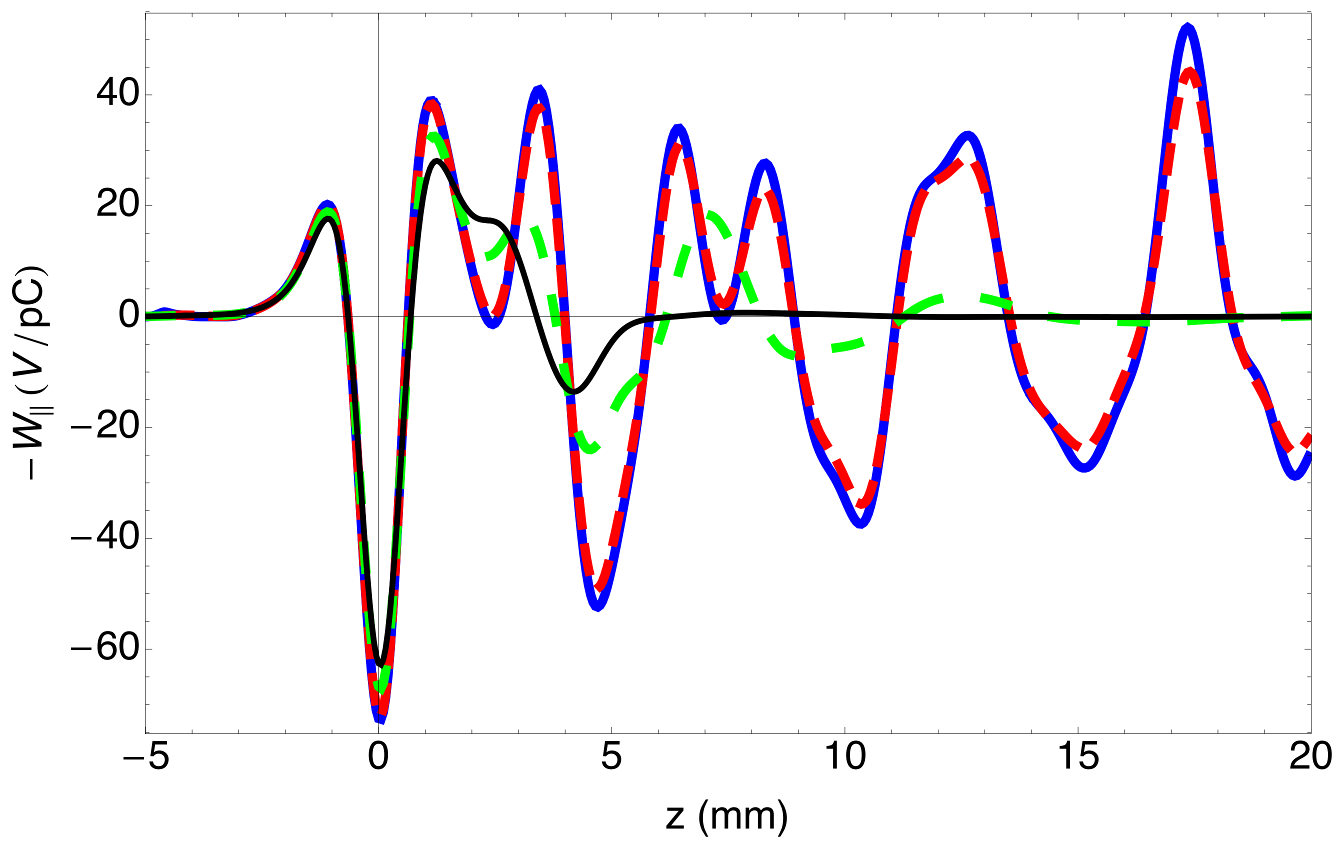

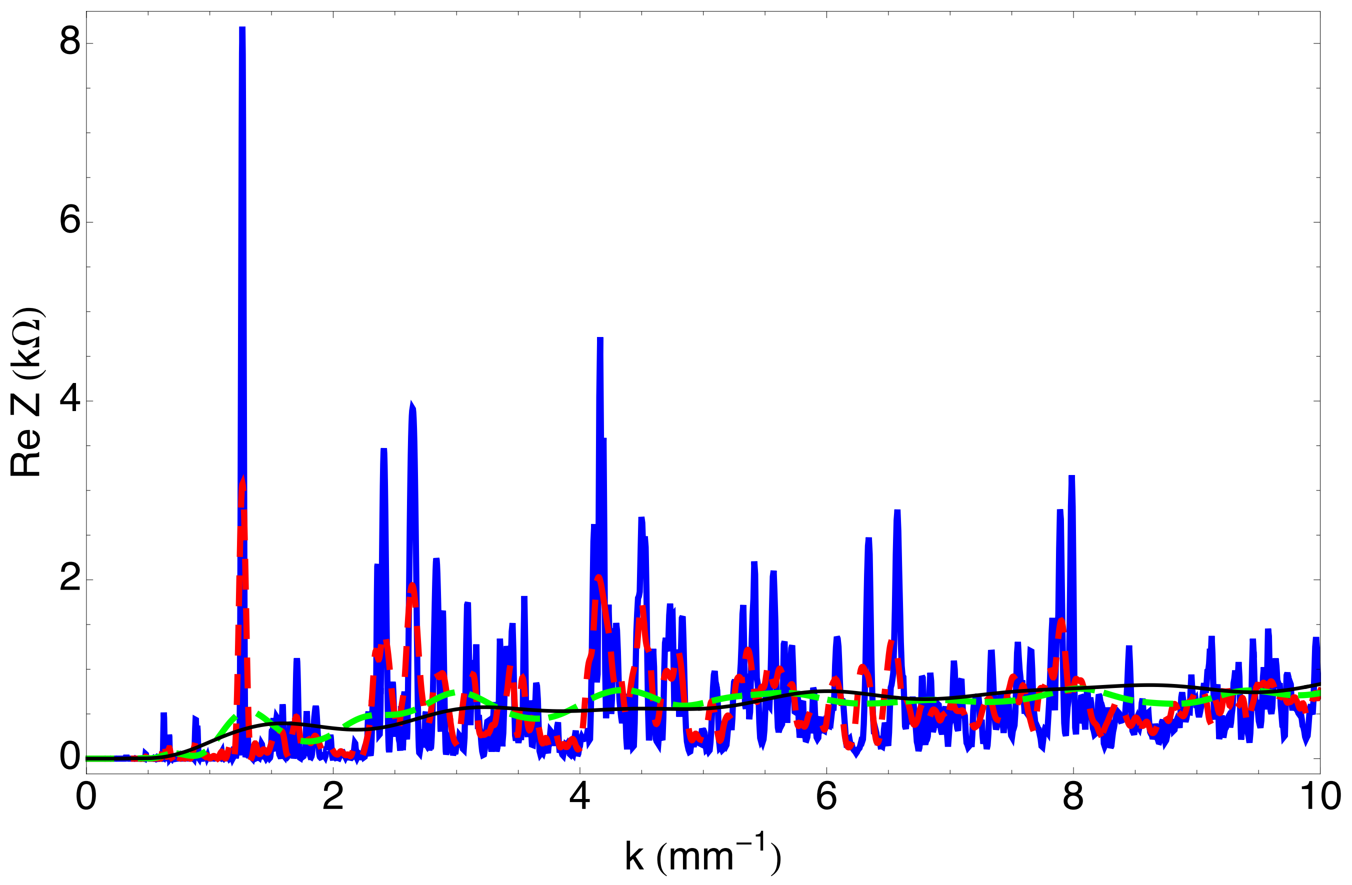

表1　立ち上げ時のマシンパラメータ. [3]

パラメータ		単位
エネルギー	1.1	GeV
周長	135	m
最大電流	12	mA
エミッタンス $(\varepsilon_x/\varepsilon_y/\varepsilon_z)$	29.9/1.50/3688	nm
放射減衰時間 $(\tau_x/\tau_y/\tau_z)$	11.5/11.7/5.9	msec
チューン $(\upsilon_x/\upsilon_y/\upsilon_s)$	8.83/6.28/0.019	
エネルギー広がり	0.055	%
バンチ長	6.7	mm
運動量圧縮率	0.01	
エネルギー損失	0.085	MV
RF 電圧	1.0	MV
RF 周波数	509	MHz
セル数	32	

[1] D. Zhou, et al., Jpn. J. Appl. Phys. 51 (2012) 016401. [2] L. Wang et al., IPAC2013, TUPME017. [3] 杉本 寛, "SuperKEKB陽電子ダンピングリングの立ち上げ", 「加速器」Vol. 15, No. 4, 2018.

CSR impedance calculation (cont'd)

- Examples of CSR impedance by CSRZ
  - NSLS VUV as an example: a/b=80/42 mm, Lbend=1.5 m, R=1.91 m (Collaboration with S. Kramer (BNL))
  - Measured SR spectrum showed similar pattern of CSR impedance [1,2,3]. This is an evidence of multi-bend interference of CSR, or CSR in "whispering gallery modes".
- Measurement of CSR wakefields and resonances
  - The principle:

$$\mathrm{Re}[Z_{\parallel}(k)] = \frac{\pi}{e^2 c}\frac{dU(k)}{dk}$$

  - Detailed measurements and simulations were done in CLS [4]

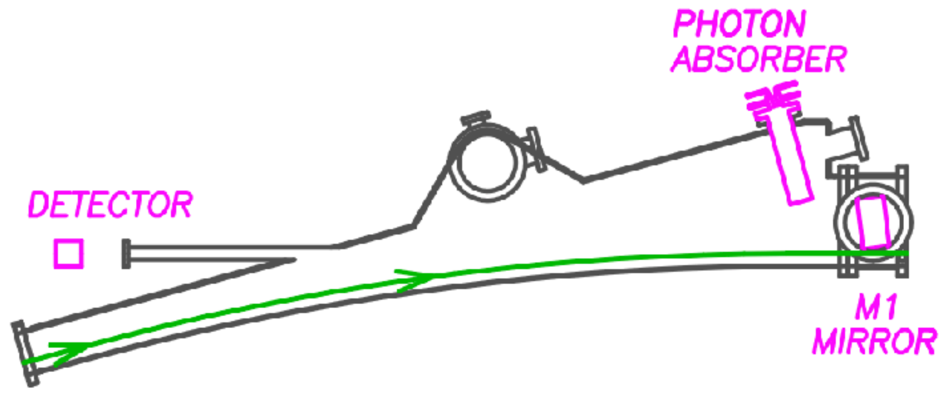

FIG. 3 (color online). Fluted vacuum chamber at the FIR dipole with bending radius $R = 7.143$ m and deflection angle $\theta = 15°$. The maximum excursion of the outer wall from the beam is 33 cm. The diode detector is at the end of the horizontal pipe at the left of the figure.

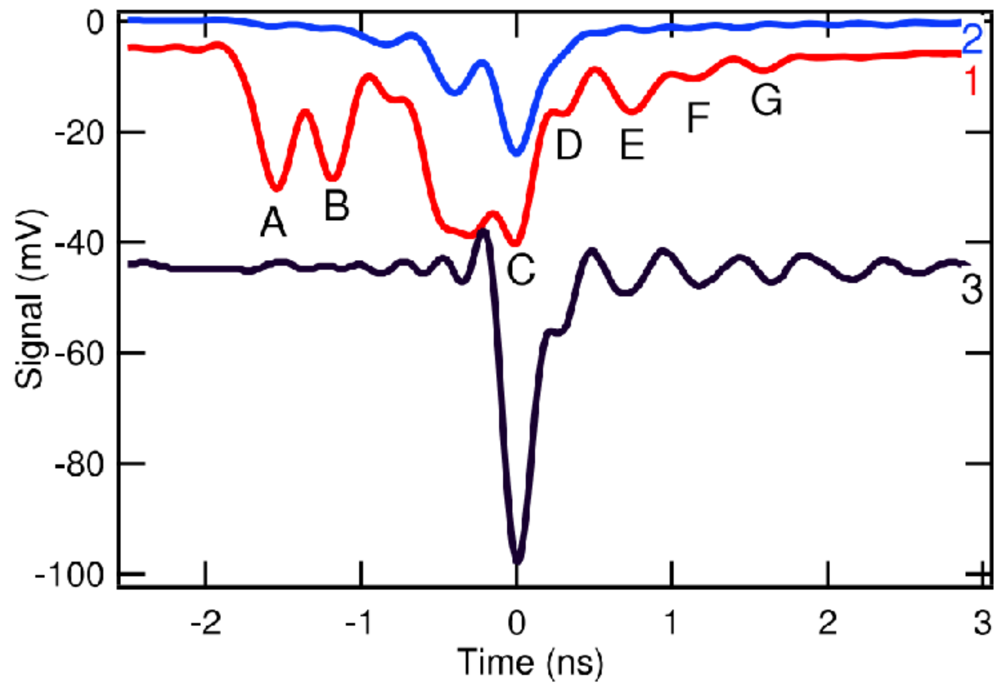

FIG. 4 (color online). rf diode measurements in the time domain (oscilloscope traces) with a 50–75 GHz detector. Diode mounting and polarization: 1—backward horizontal; 2—backward vertical; 3—forward horizontal (with adjustment of time base). For clarity the curves have been separated vertically.

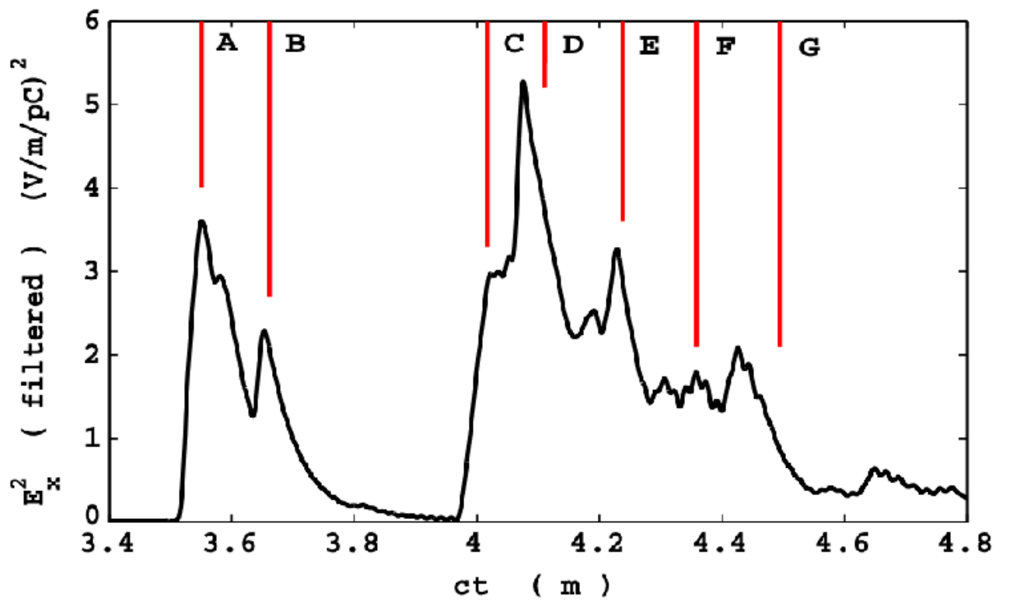

FIG. 5 (color online). Simulated E_x^2 at backward port vs ct, after a low pass filter to account for detector response. The origin of time t is when the bunch is 5 cm before the entrance to the bend. Only the lowest mode in y is included.

First explanation of CSR resonances (experiment in CLS) [4]

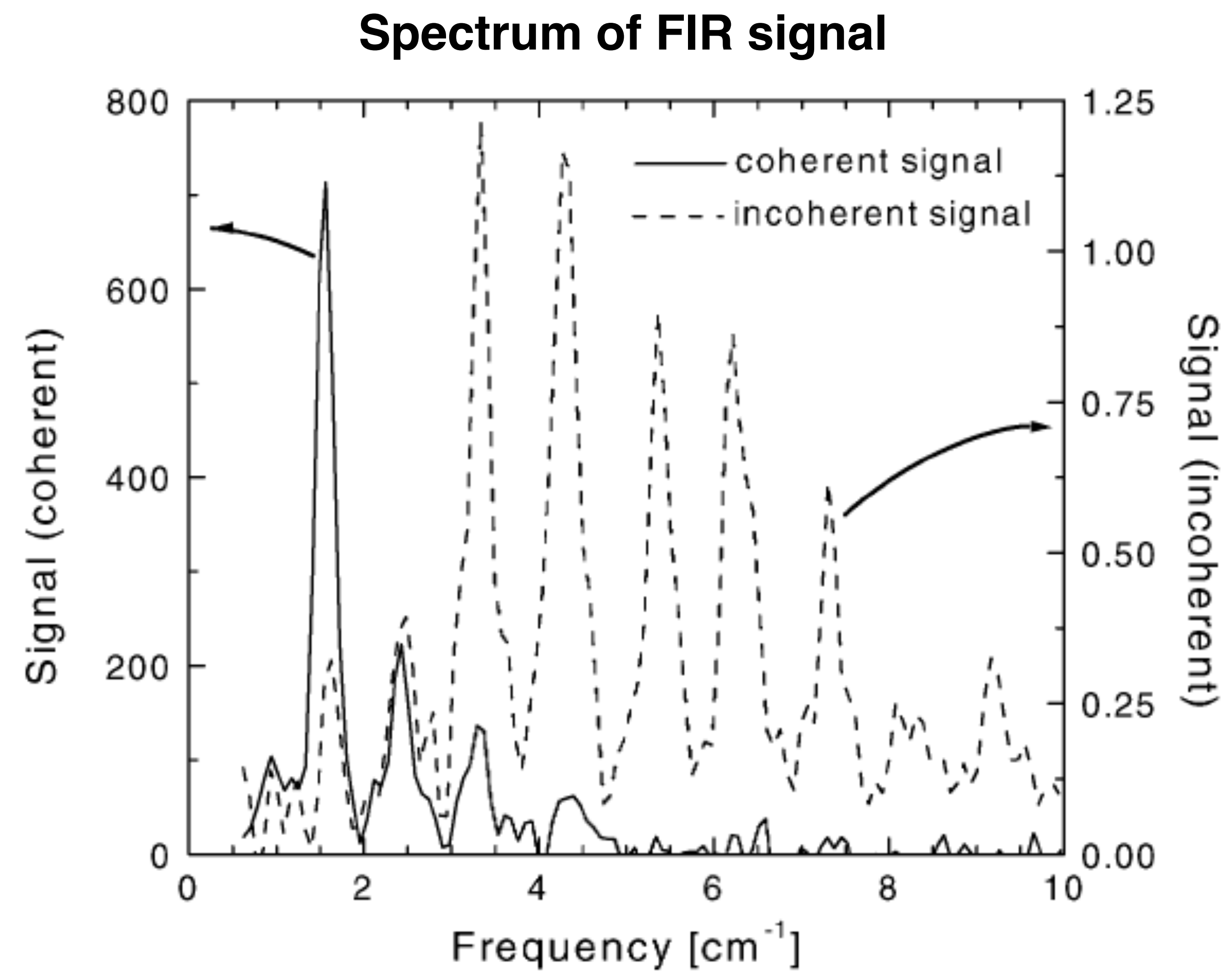

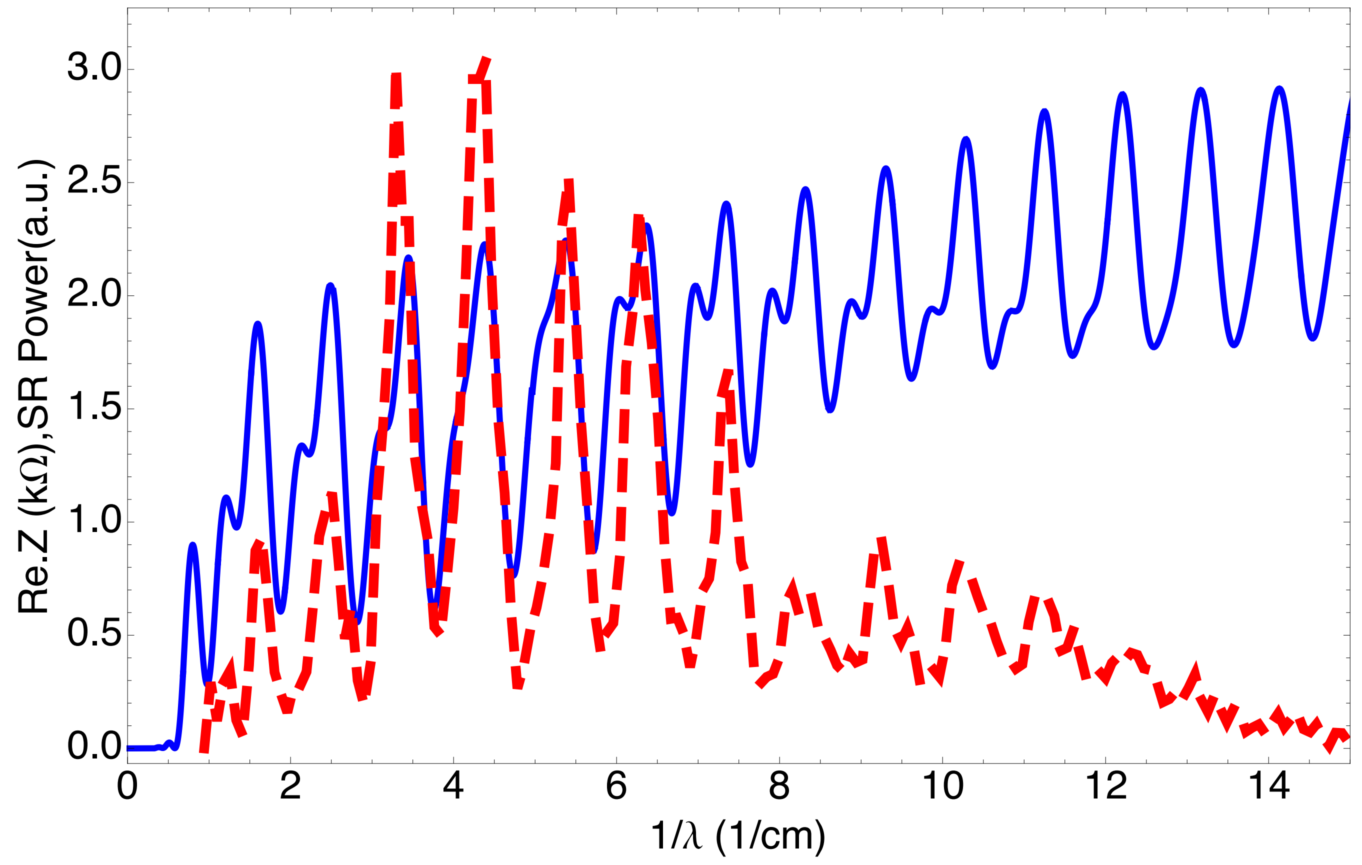

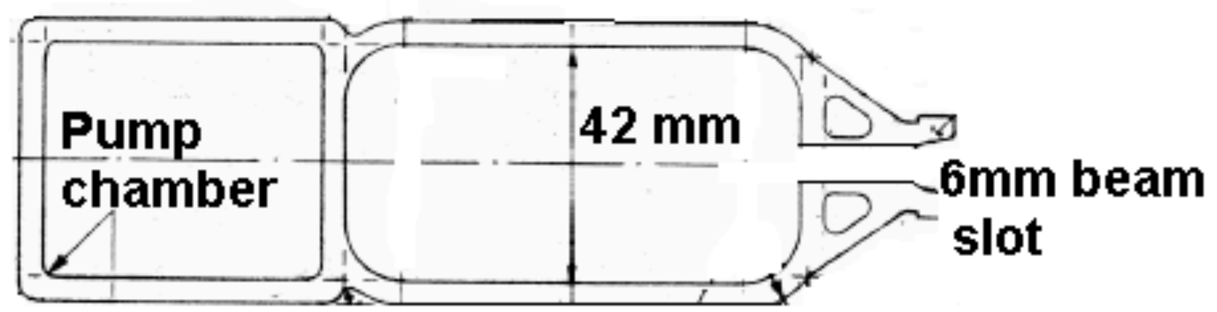

CSR signals in NSLS-VUV [3,2]

[1] D. Zhou, IPAC'12, MOOBB03. [2] R. Warnock, arXiv:1708.05500. [3] G. Carr et al., NIM-A 463, 387 (2001). [4] B.E. Billinghurst et al., Phys. Rev. Lett. 114, 204801 (2015).

CSR impedance calculation (cont'd)

- Examples of CSR impedance by CSRZ
  - CSR in a wiggler/undulator: Coherent wiggler/undulator radiation (CWR/CUR).
  - The CWR spectrum can be calculated analytically (for example, see Refs.[1,2]):

$$\mathrm{Re}\ Z(k) = \frac{4Z_0}{abR_0^2}\sum_{m=0}^{\infty}\sum_{p=1}^{\infty}\frac{k}{(1+\delta_{m0})k_z}\frac{\sin^2((k-k_z-k_w)L_w/2)}{(k-k_z)^2-k_w^2}$$

  - A weak wiggler: a/b=100/20 mm, λw=1 m, R0=100 m, N_{period}=10
  - Blue line by CSRZ; Red line by analytic theory with rectangular chamber; Green line by analytic theory in free space [3].

$$Z(k) = \frac{1}{4}Z_0 L_w k\frac{k_w}{k_0}\left(1-\frac{2i}{\pi}\left(\log\frac{4k}{k_0}+\gamma_E\right)\right)$$

  - For storage-ring light sources or THz FELs, it might be interesting to look at the interference of CUR + SC + RW.

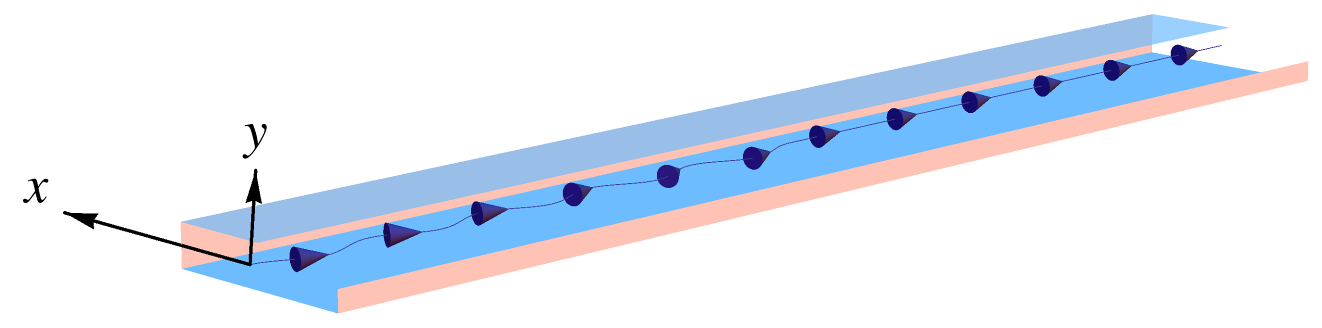

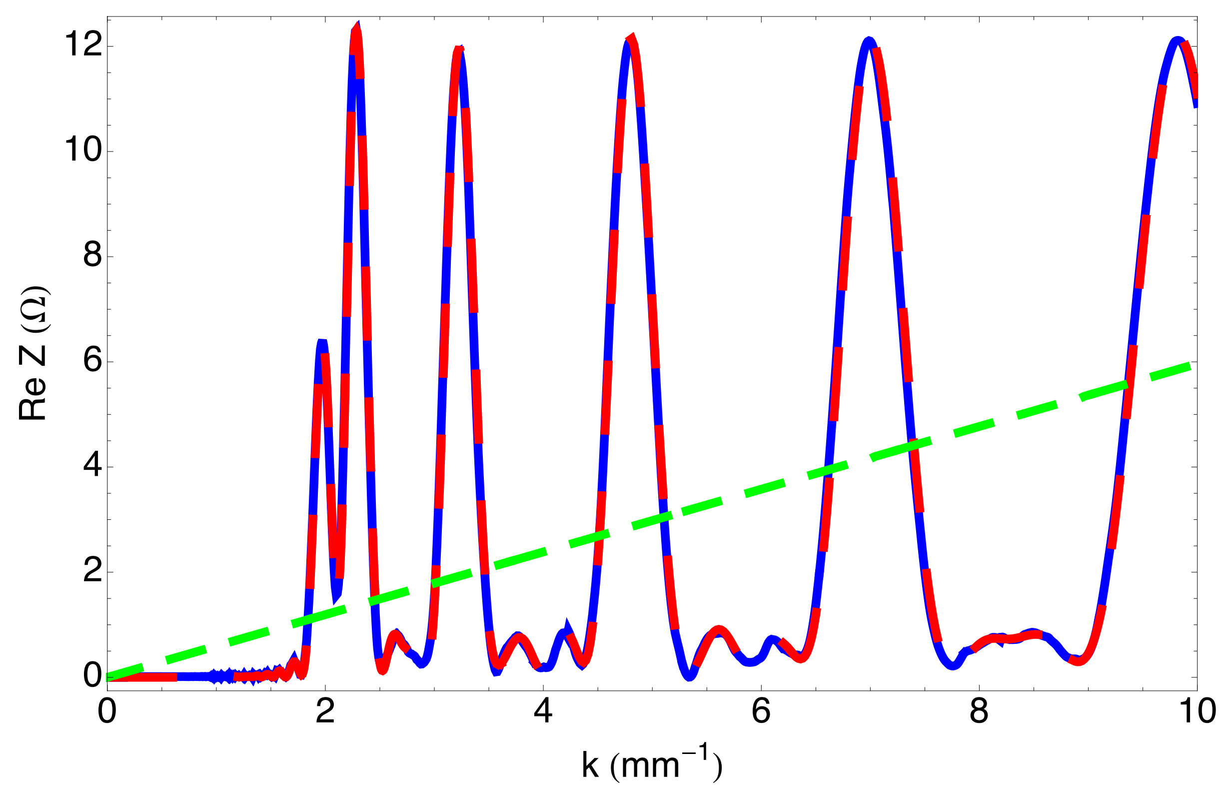

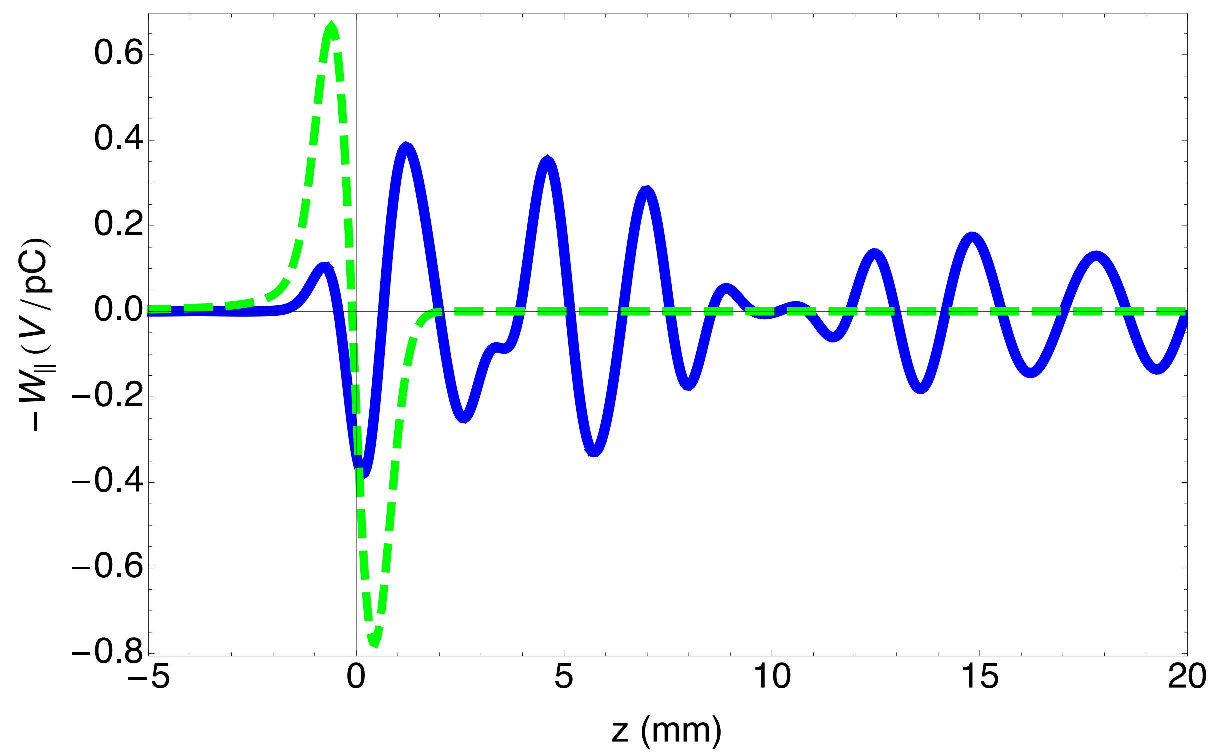

- Question: Measurements of CWR/CUR signals?

[1] Y. Chin, LBL-29981, 1990. [2] G. Stupakov and D. Zhou, KEK Preprint 2010-43. [3] J. Wu et al., Phys. Rev. ST Accel. Beams **6**, 040701 (2003).

Analytic theories of CSR driven MWI threshold

- Stupakov-Heifets (S-H) theory [1] on CSR instability
  - Beam becomes unstable when $(\pi R/(2h))^{3/2} \le kR < 2\Lambda^{3/2}$.
  - For Gaussian bunch, the theory is valid when $k\sigma_z \gg 1$ (coasting-beam approximation).
  - The S-H theory was translated to bunch current threshold [2]:

$$1 = \frac{i r_0 c Z(k)}{\gamma} \int \frac{d\delta\,(d\rho_0/d\delta)}{\omega + ck\eta\delta} \quad \rightarrow \quad I_b > \frac{\pi^{1/6}}{\sqrt{2}} \frac{ec}{r_0} \frac{\gamma}{\rho^{1/3}} \alpha_p \delta_0^2 \sigma_z \frac{1}{\lambda^{2/3}}$$

- Improvements on S-H theory
  - Simulation of MWI with steady-state parallel-plates model of CSR impedance [3].

$$I_{\text{th1}} = \frac{4\pi(E/e)\eta\sigma_\delta^2\sigma_z^{1/3}}{Z_0\rho^{1/3}} S_{\text{th1}} \qquad S_{\text{th1}} \approx 0.5 + 0.12\Pi \qquad \Pi \equiv \sigma_z\sqrt{\rho/h^3}$$

  - This scaling law was well validated by simulations and experiments [4]. But note that this is only true when CSR dominates the instability.
  - Simulation of MWI with steady-state rectangular-chamber model of CSR impedance [5].

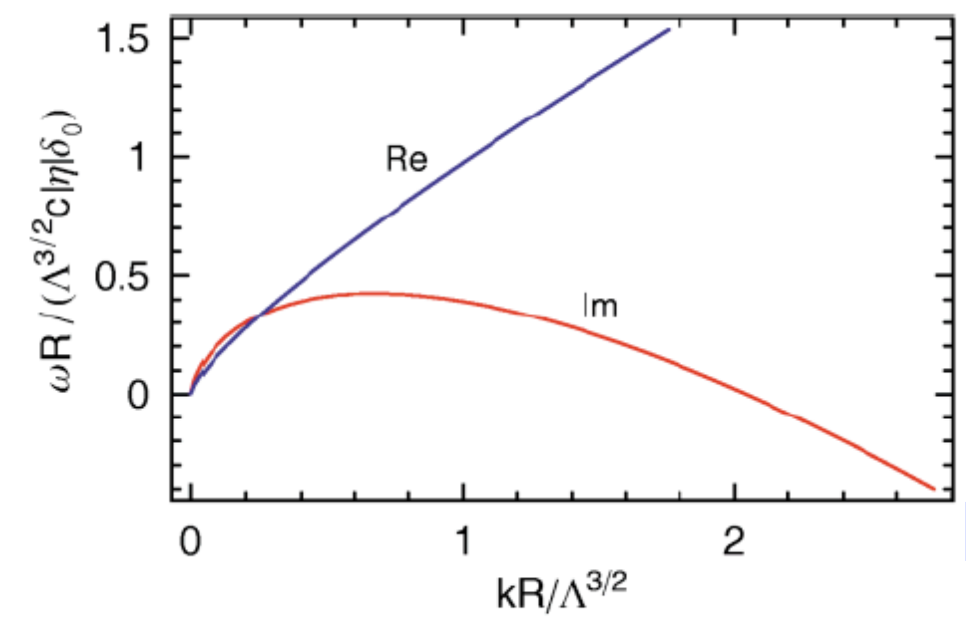

[1]

FIG. 1. (Color) The imaginary (Im) and real (Re) parts of the frequency ω as functions of $kR/\Lambda^{3/2}$, for a positive value of η. For negative values of k, the frequency can be found from the relation $\omega(-k) = -\omega^*(k)$ which follows from Eq. (9).

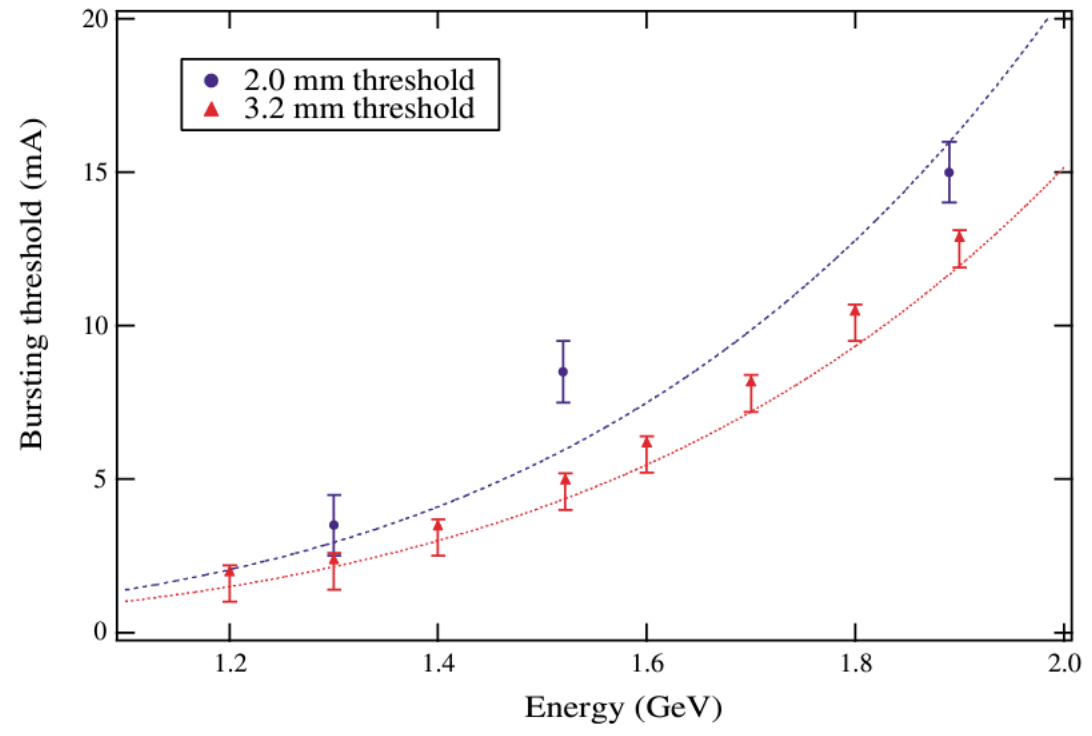

First observation of CSR burst in e-ring [2]

FIG. 4 (color online). Bursting threshold as a function of electron beam energy at 3.2 and 2 mm wavelengths. Data are shown as points. Calculated threshold using nominal ALS parameters at 3.2 and 2 mm wavelengths are shown as dashed lines.

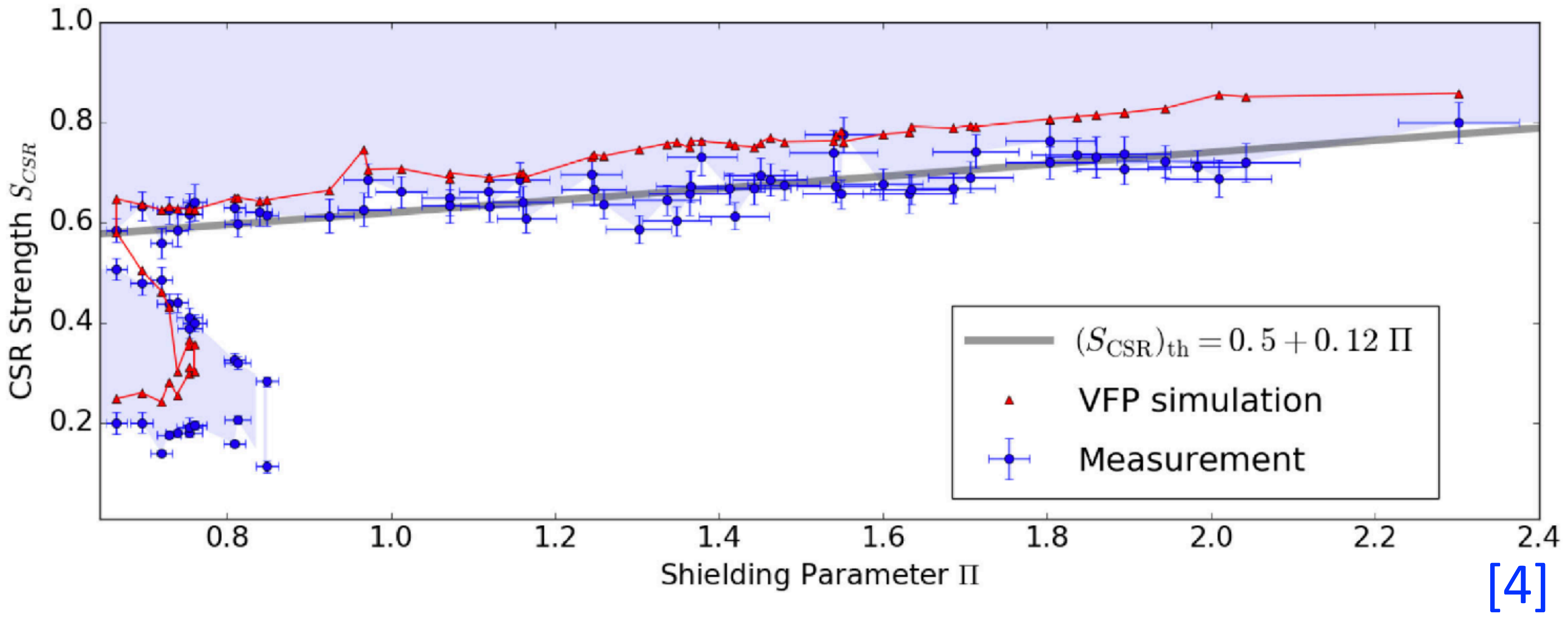

[4]

[1] G. Stupakov and S. Heifets, PRST-AB 5, 054402 (2002). [2] J. Byrd, et al., PRL 89, 22, Nov. 2002. [3] K.L. F. Bane, Y. Cai, and G. Stupakov, PRST-AB **13**, 104402 (2010).
[4] M. Brosi et al., PRAB 22, 020701 (2019). [5] Y. Cai, Phys. Rev. ST Accel. Beams **17**, 020702 (2014).

Analytic theories of CSR driven MWI threshold (cont'd)

- The case of arbitrary impedance $Z(k)$
  - An alternative way of extending S-H theory is to solve the dispersion relation numerically with $A = \Omega/(ck\eta\sigma_p)$ [1]:

$$-if(I_b)\frac{Z_{\parallel}(k)}{k}G(A) = 1$$

$$G(A) = \int_{-\infty}^{\infty} dp \frac{pe^{-p^2/2}}{A+p} \qquad f(I_b) = \frac{I_b}{2\pi(E/e)\eta\sigma_p^2\sigma_z}$$

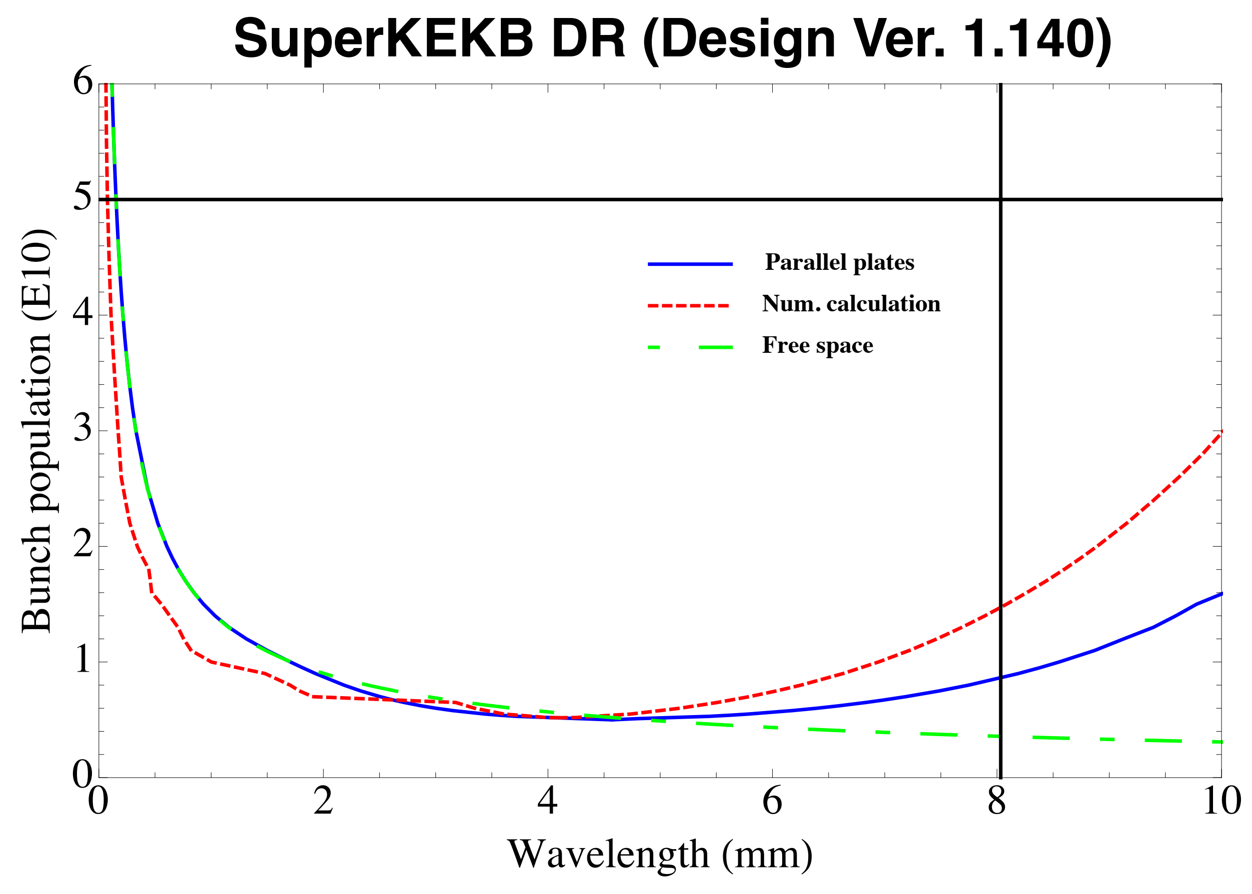

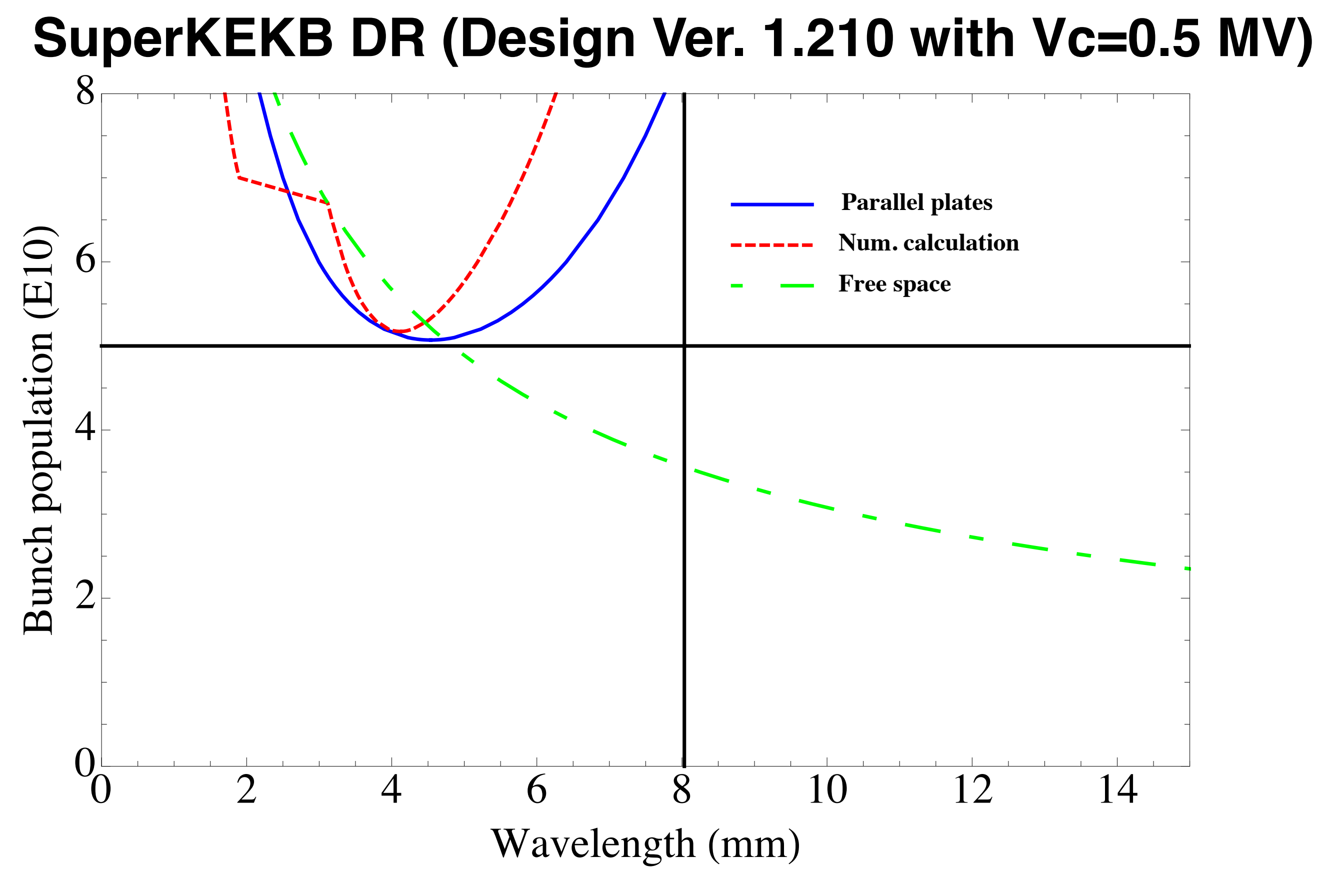

  - The impedance $Z(k)$ can be obtained by analytical or numerical methods, including transient effects and/or chamber shielding.
  - For the impedance $Z(k)$, it is good to use data as a smooth function of k (broadband impedance).
  - For CSR impedance in storage rings, the low-frequency part of $Z(k)$ is mainly determined by chamber shielding, the high-frequency part is mainly determined by transient effects.
  - For SuperKEKB damping ring, the design had to be changed due to strong CSR instability

[1] D. Zhou et al., "CSR in the SuperKEKB Damping Ring", in Proceedings of IPAC'10, Kyoto, Japan.

Analytic theories of CSR driven MWI threshold (cont'd)

- The case of arbitrary impedance $Z(k)$
  - Further simplification of the dispersion-relation problem with threshold condition Im[Ω]=0 [1]:

$$G(A) = \int_{-\infty}^{\infty} dp \frac{p e^{-p^2/2}}{A+p} = \sqrt{2\pi} + i\pi A e^{-\frac{A^2}{2}} \left[\mathrm{sgn}[\mathrm{Im}[A]] + i\,\mathrm{erfi}\left[\frac{A}{\sqrt{2}}\right]\right]$$

$$G_r(A_r) = \sqrt{2\pi} - \pi A_r e^{-A_r^2/2}\mathrm{erfi}[A_r/\sqrt{2}] \qquad G_i(A_r) = \mathrm{sgn}[\eta]\pi A_r e^{-A_r^2/2}$$

$$\frac{G_i(A_{th})}{G_r(A_{th})} = \frac{Z_r(k)}{Z_i(k)} \qquad \frac{I_{th}}{2\pi(E/e)\eta\sigma_\delta^2\sigma_z} = \frac{kZ_r}{G_i(A_{th})(Z_r^2+Z_i^2)}$$

→ Roughly, $I_{th} \propto 1/(Z_{\parallel}/n)$

  - **Application-1**: Scaling law of Coherent Wiggler Radiation (CWR) instability in damping rings (only valid for positive η):

$$I_b^{th}(\lambda) \approx \frac{8\pi\sqrt{2\pi}(E/e)\eta\sigma_p^2\sigma_z}{LZ_0\theta_0^2 \ln\frac{2k_w\lambda}{\pi\theta_0^2}}$$

  - This scaling law well explains the simulated CWR instability in the ring cooler for EIC [1, 2].

TABLE I. Preliminary damping wiggler parameters for the EIC backup ring cooler.

Magnetic field, B	T	1.9
Length, L	m	7.44
Bending radius, ρ	m	0.246
Wiggler period, λ_w	mm	48
Number of poles, N_p		155
Vertical full chamber height, b	mm	15
Horizontal full chamber width, a	mm	45
Number of DWs, N_w		16

TABLE II. Main ring cooler parameters.

Energy, E_0	MeV	149.26
Circumference, C	m	426
Momentum compaction, α_c		-3.21×10^{-3}
Revolution period, T_0	μs	1.42
Energy loss, U_0	keV	5.933
Synchrotron tune, ν_s		0.0029
Damping time, σ_x, σ_τ	ms	31.7, 15.71
rf voltage, V_{rf}	kV	19
rf frequency, f_{rf}	MHz	98.5233
Harmonic number, h		140
Energy spread, σ_δ		6.5×10^{-4}
Bunch length, σ_s	mm	48

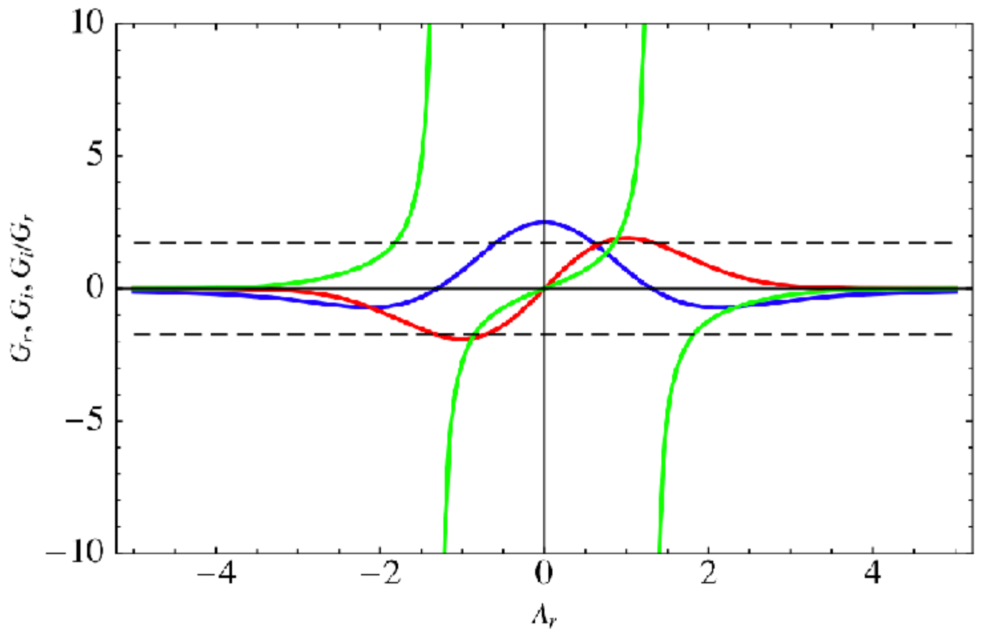

FIG. 13. The functions $G_r(A_r)$ (blue line), $G_i(A_r)$ (red line), and $G_i(A_r)/G_r(A_r)$ (green line) with real A_r and positive η. The horizontal dashed lines indicate $G_i/G_r = \pm\sqrt{3}$.

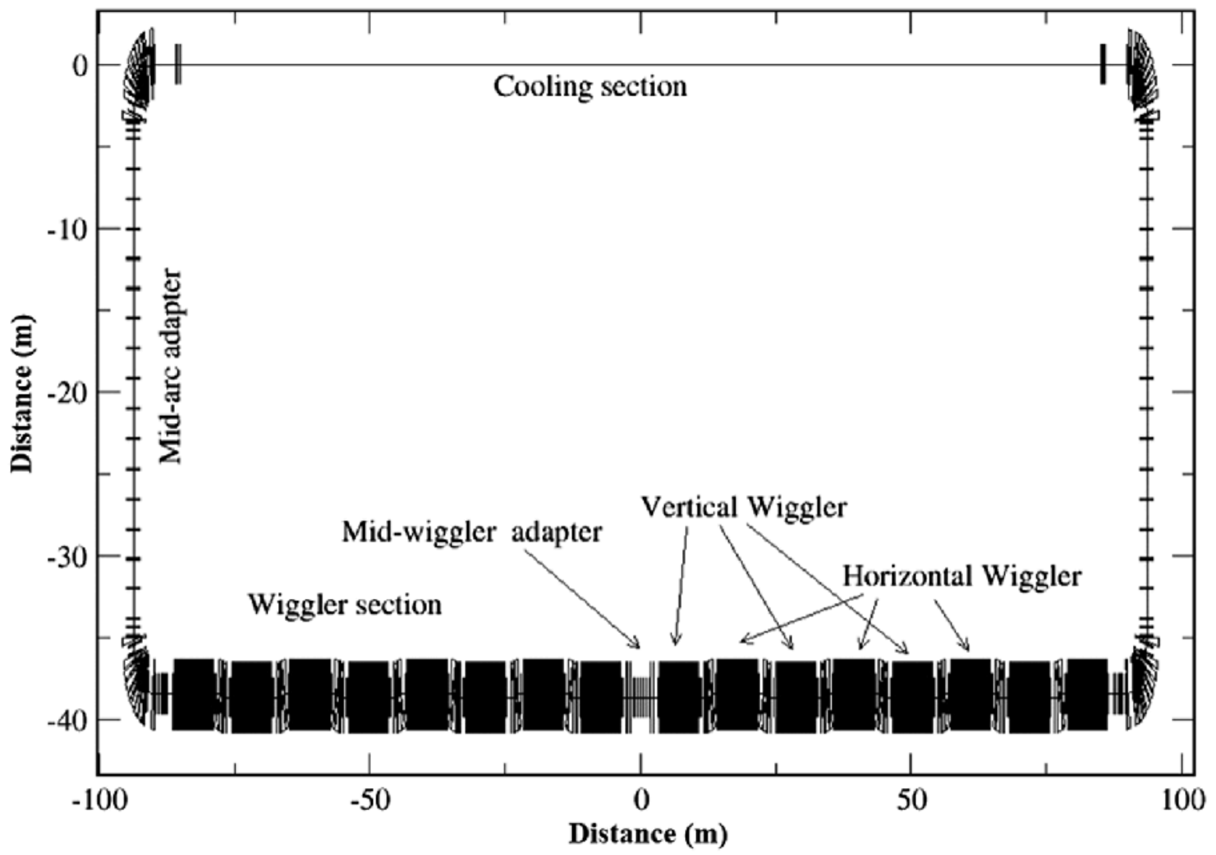

Theory

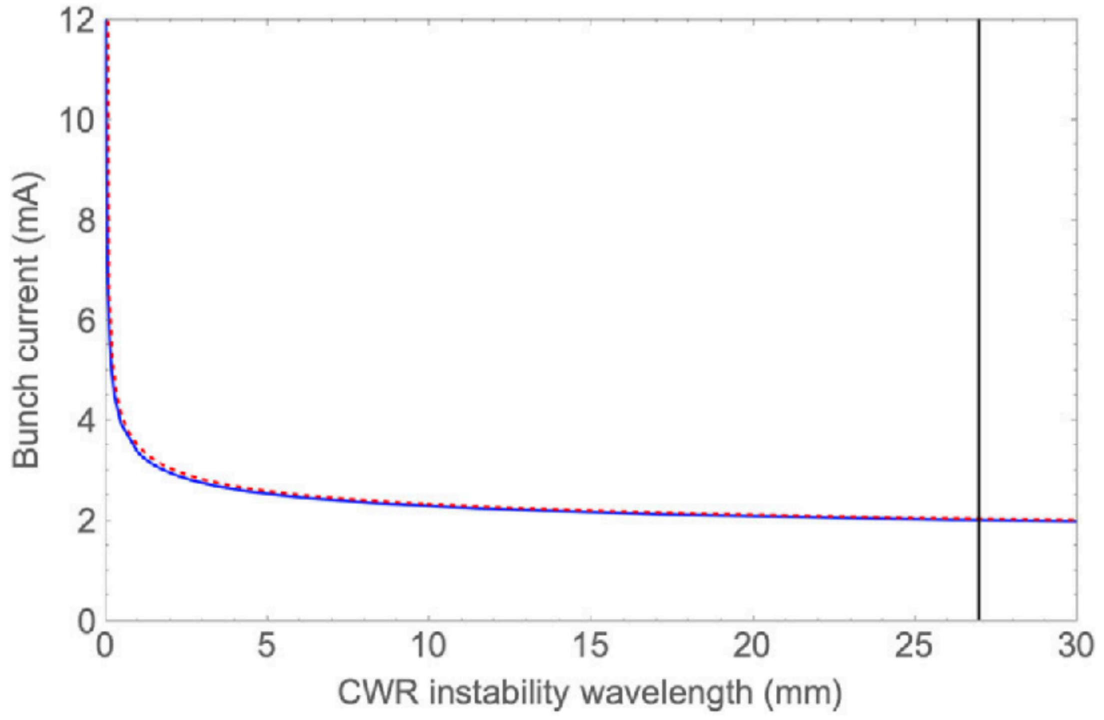

VFP simulation (R. Lindberg)

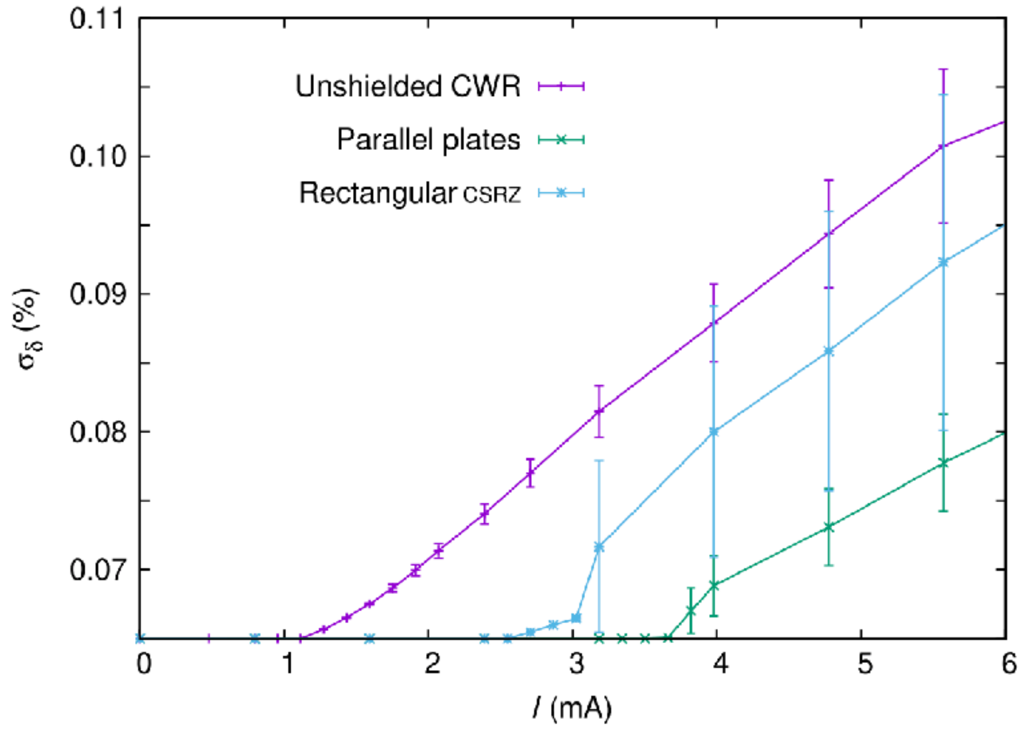

[1] A. Blednykh et al., Phys. Rev. Accel. Beams **26**, 051002 (2023). [2] H. Zhao et al., Phys. Rev. Accel. Beams **24**,043501(2021)

Analytic theories of CSR driven MWI threshold (cont'd)

- The case of arbitrary impedance $Z(k)$
  - **Application-2**: Scaling law of CSR instability with parallel-plates steady-state model [1]:

$$I_{\text{th2}} = \frac{4\pi(E/e)\eta\sigma_\delta^2\sigma_z^{1/3}}{Z_0\rho^{1/3}} S_{\text{th2}} \qquad S_{\text{th2}} \approx 0.384\Pi^{2/3} \qquad \Pi \equiv \sigma_z\sqrt{\rho/h^3}$$

  - This scaling law (first found by Y. Cai [2]) is valid when $\Pi \gg 0.5$. It suggests CSR threshold is proportional to $\gamma\eta\sigma_\delta^2\sigma_z^{4/3}$, but independent of ρ [2].
  - The linear scaling law of S_{th1} is an approximation of S_{th2}.
  - **Application-3**: Scaling law of Resistive Wall (RW) instability [1]:

$$Z_\parallel^{\text{RW}}(k) = \frac{f_Y Z_0 L_{\text{RW}}}{\pi h\left(2\sqrt{\frac{iZ_0\sigma_c}{k}} - ihk\right)} \qquad \chi = \frac{\sqrt{2Z_0\sigma_c}}{hk^{3/2}}$$

$$I_{\text{th}} = \frac{2\pi^2(E/e)\eta\sigma_\delta^2\sigma_z(2Z_0\sigma_c h)^{2/3}}{f_Y Z_0 L_{\text{RW}}}\text{Min}[Y_{\text{th}}(\chi)] \qquad Y_{\text{th}}(\chi) = \frac{1}{G_{\text{i}}(A_{\text{th}})\chi^{1/3}}$$

  - $\text{Min}[Y_{\text{th}}(\chi)] \approx 0.566$. The scaling law is valid when

$$\Pi_{\text{RW}} \equiv \sigma_z\left(\frac{Z_0\sigma_c}{h^2}\right)^{1/3} \gg 0.73$$

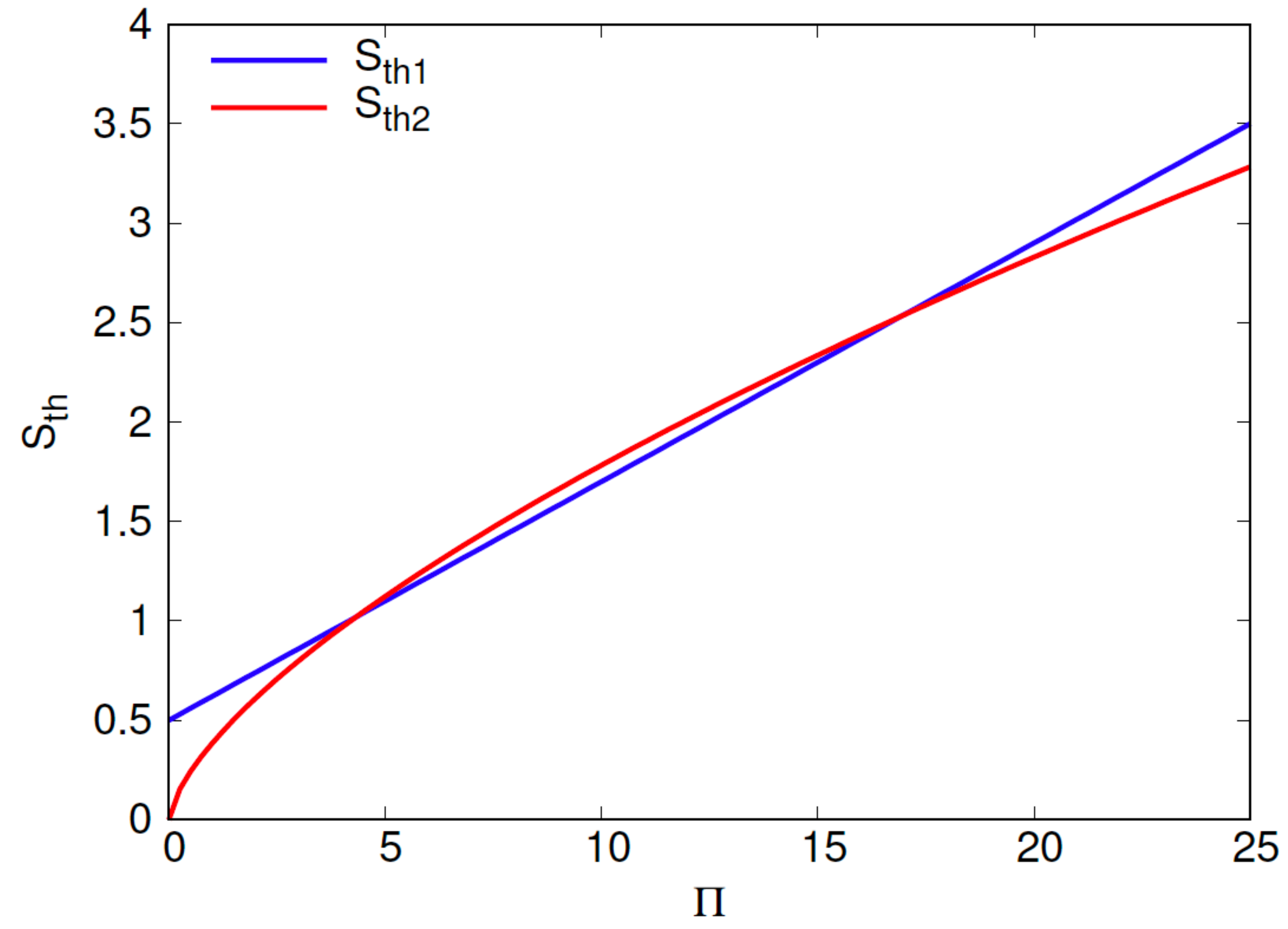

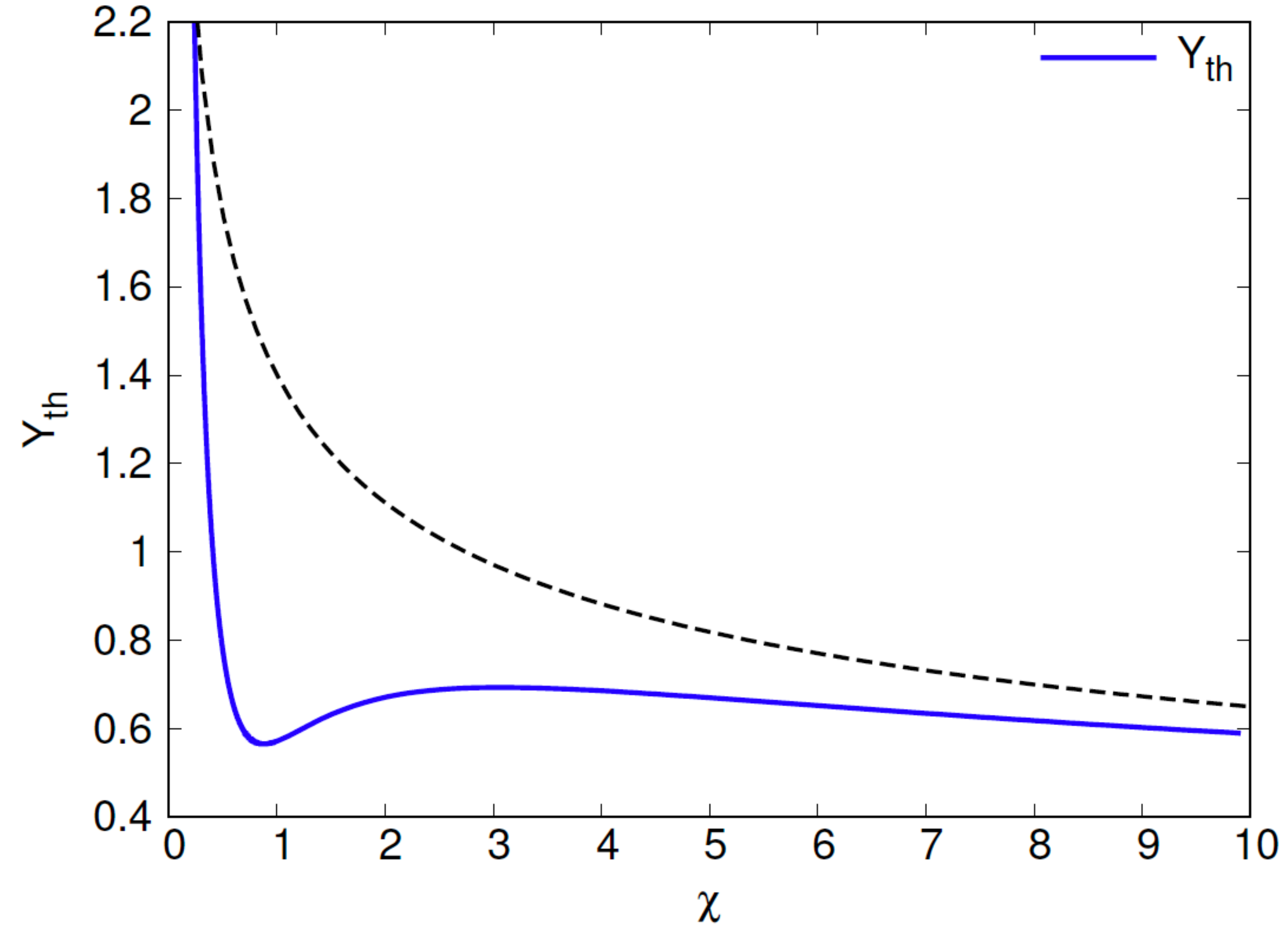

[1] S. Dastan, D. Zhou et al., to be published. [2] Y. Cai, IPAC2011, FRXAA01.

Prediction of CSR instability via simulations

- **Check list** before running simulations
  - Scaling law with PP-SS CSR model:
$$I_{\text{th2}} = \frac{4\pi(E/e)\eta\sigma_\delta^2\sigma_z^{1/3}}{Z_0\rho^{1/3}}S_{\text{th2}}$$
→ Global picture
  - Critical wavenumber: $k_c = 3\gamma^3/(2\rho)$. Interaction distance of CSR: $z \gg 1/k_c$.
  - Wall shielding threshold: $k_w = \pi\sqrt{\rho/(2h)^3}$. When $\sigma_z \ll 1/k_w$, wall shielding is not crucial; when $\sigma_z \gg 1/k_w$, wall shielding becomes important (according to $S_{\text{th1}} \approx 0.5 + 0.11\sigma_z k_w$).
  - NOTE: $\sigma_z \gg 1/k_w$ does not mean CSR is negligible. In theory, there always is a finite I_{th} for any $\sigma_z k_w$.
  - Critical CSR wavenumber: $k_{\text{th}} = 2\sqrt{\rho/h^3} \sim 2k_w$. CSR around k_{th} determines the threshold current.
  - Radiation formation length: $l_f = (24\rho^2\sigma_z)^{1/3}$. For long magnet $l_b \gtrsim l_f$, transient effects are negligible; for short magnet $l_b < l_f$, transient effects become significant.
  - Catch-up distance: $l_c = 2\sqrt{2\rho w}$ with w the distance from the beam orbit to the side wales and path difference $\Delta s = \frac{4}{3}\sqrt{\frac{2w^3}{\rho}}$. When $\Delta s \lesssim \sigma_z$, reflected CSR plays a role.
  - Slippage length: $l_s = \eta\sigma_\delta C$. Lumping the CSR impedance of distributed bends into one point is valid only when $l_s \ll \lambda_{\text{CSR}}$.

→ Proper choices of Impedance models
→ Proper setup of simulations

Prediction of CSR instability via simulations (cont'd)

- Example-1: SuperKEKB LER
  - Step-1: Impedance modeling of CSR/CWR by CSRZ, RW by IW2D, and geometric wakes by GdfidL, CST, and ECHO3D [1].
  - Step-2: Instability analysis to determine $I_{\rm th}(k)$.
  - Step-3: Choosing important parameters: maximum $k_{\rm max}$ for impedance model, minimum mesh size $\Delta z \ll 2\pi/k_{\rm max}$.
    - $k_{\rm max}$=6 mm^{-1} $\rightarrow$ $f_{\rm max}$=286 GHz.
  - Note: Be careful in choosing filtering function to damp high-frequency impedances.

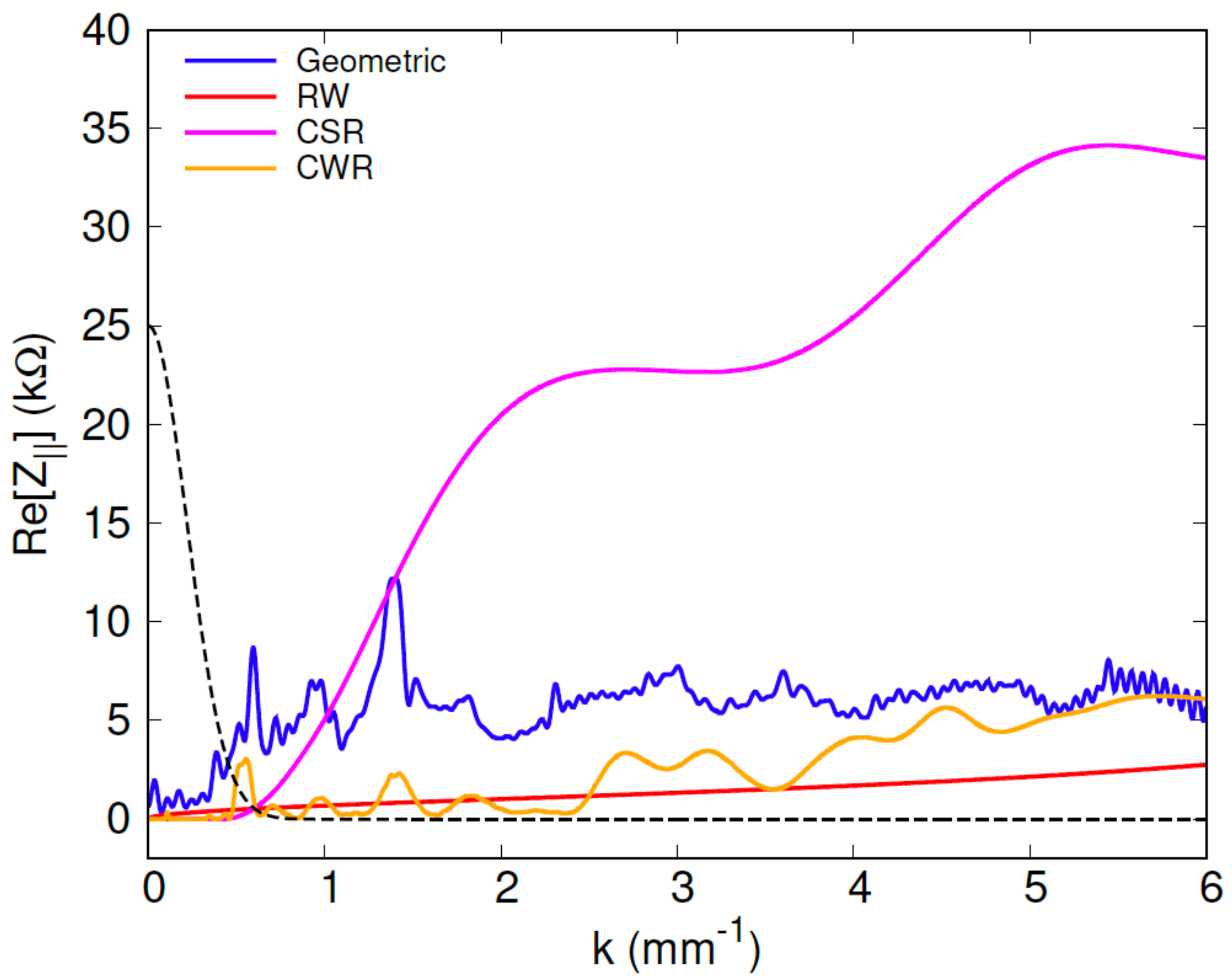

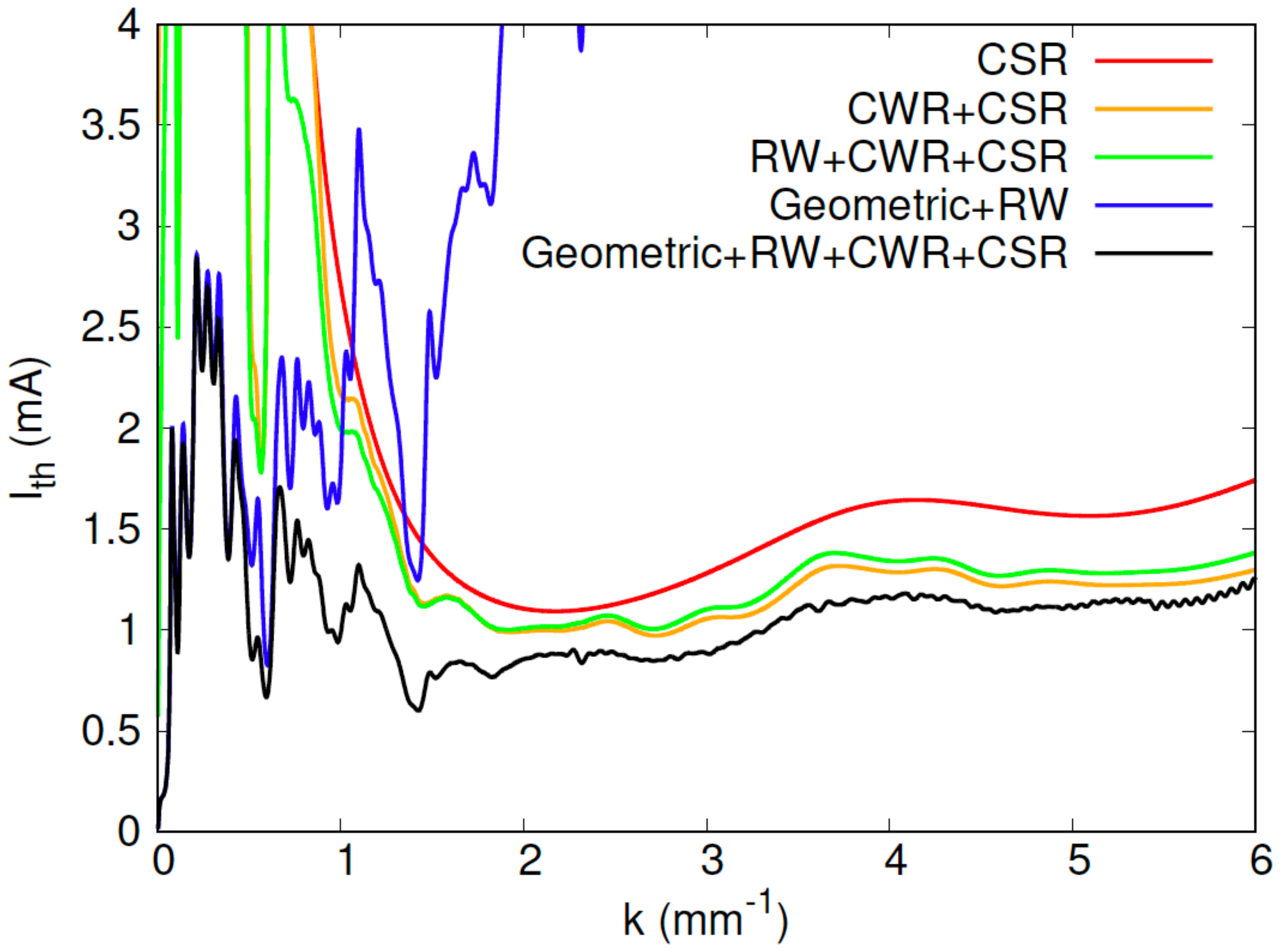

CSR is important source for MWI in SuperKEKB LER

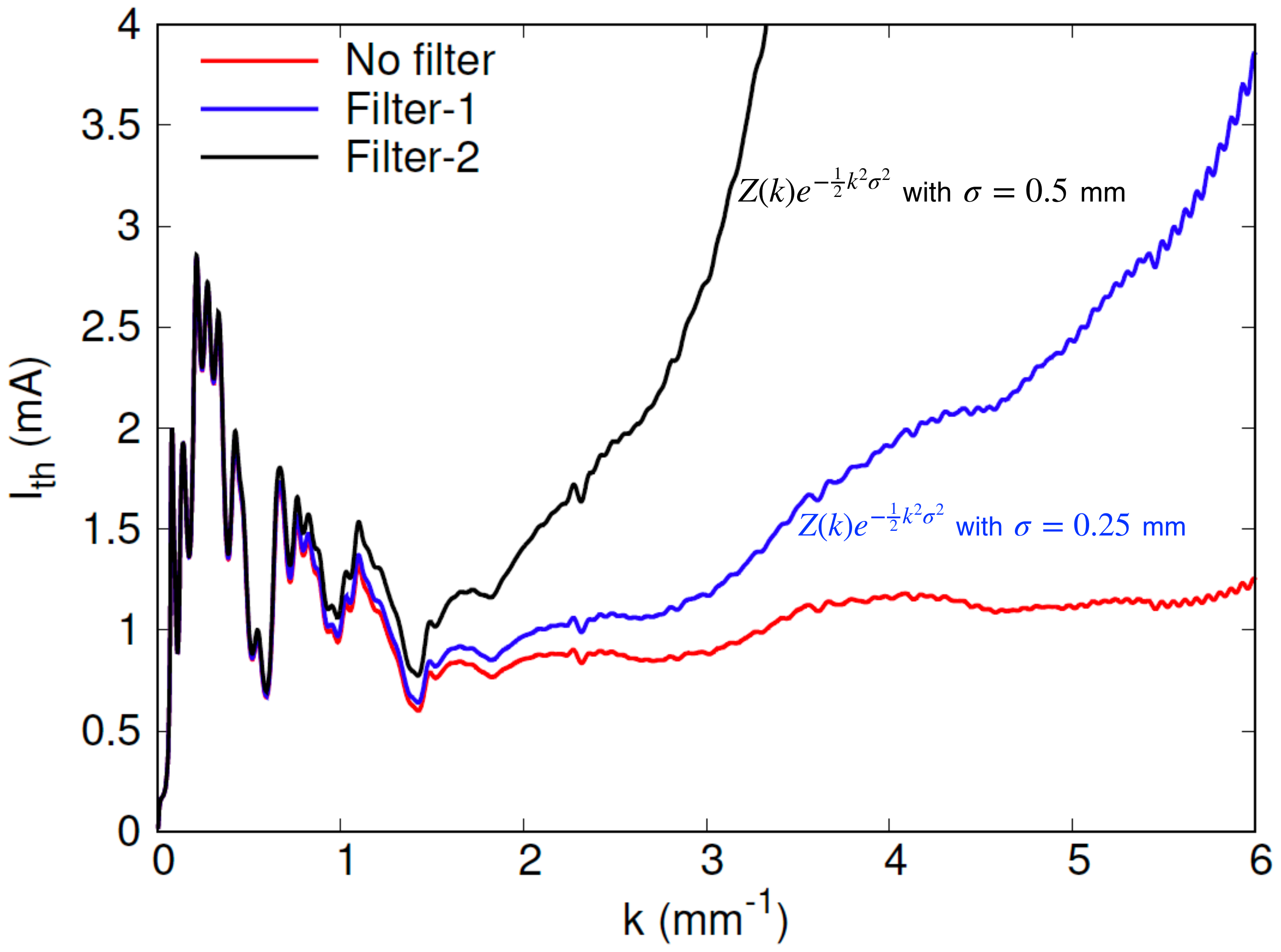

Filtered impedance models underestimate MWI threshold

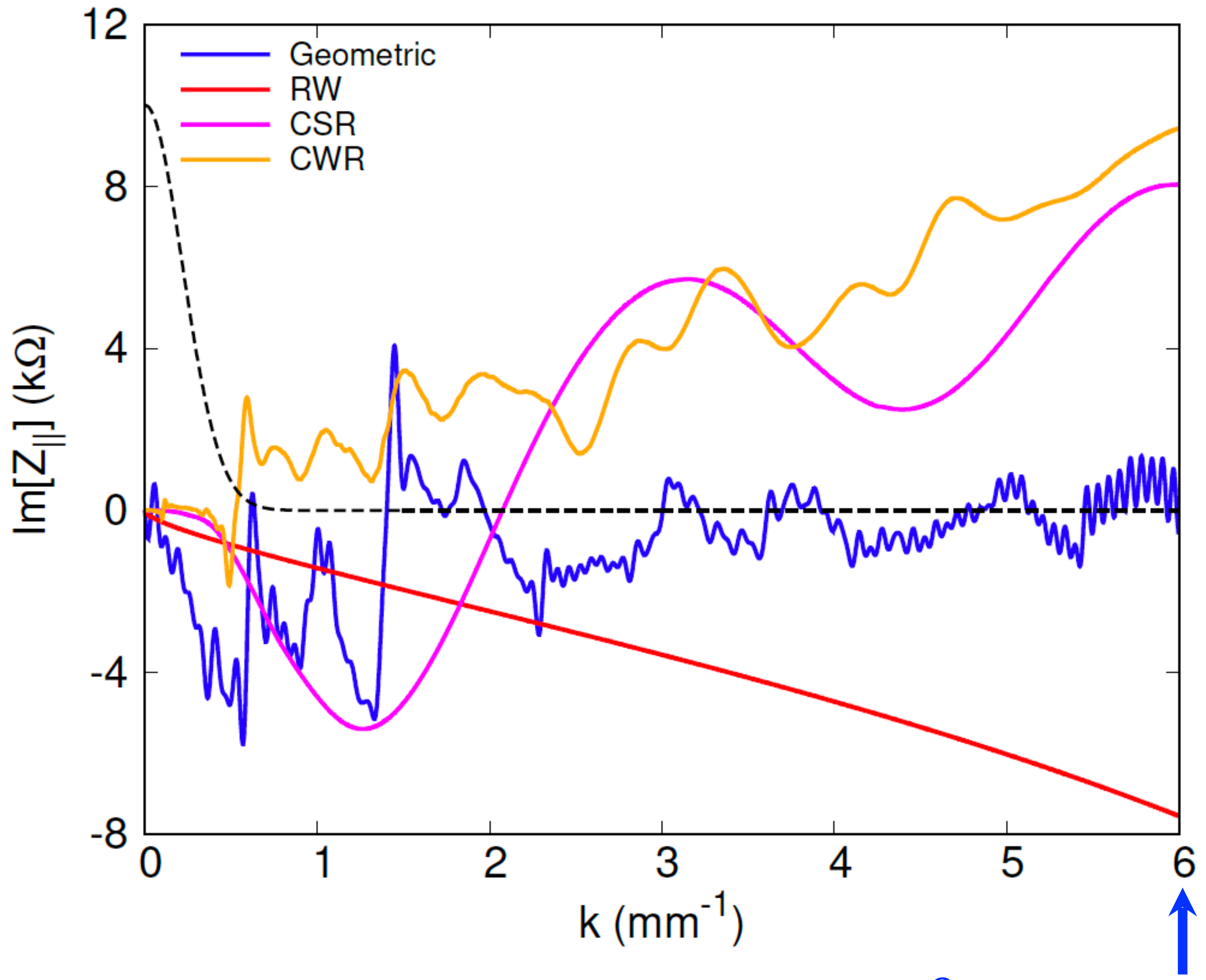

$f_{\rm max}$=286 GHz

[1] T. Ishibashi et al 2024 JINST 19 P02013.

Prediction of CSR instability via simulations (cont'd)

- Example-1: SuperKEKB LER
  - Step-4: Run VFP simulations.
    - Different combinations of impedance sources: CSR sets MWI threshold
    - Different filtering functions for impedance model
  - Step-5: Check consistency between theories and simulations.
    - "Numerical arts": Interpolation, smoothing histogram, mesh size, number of wake kicks per turn, mesh boundaries, cutoff of impedance beyond k_{max}, …
    - A good simulation should be well understood by a good theory

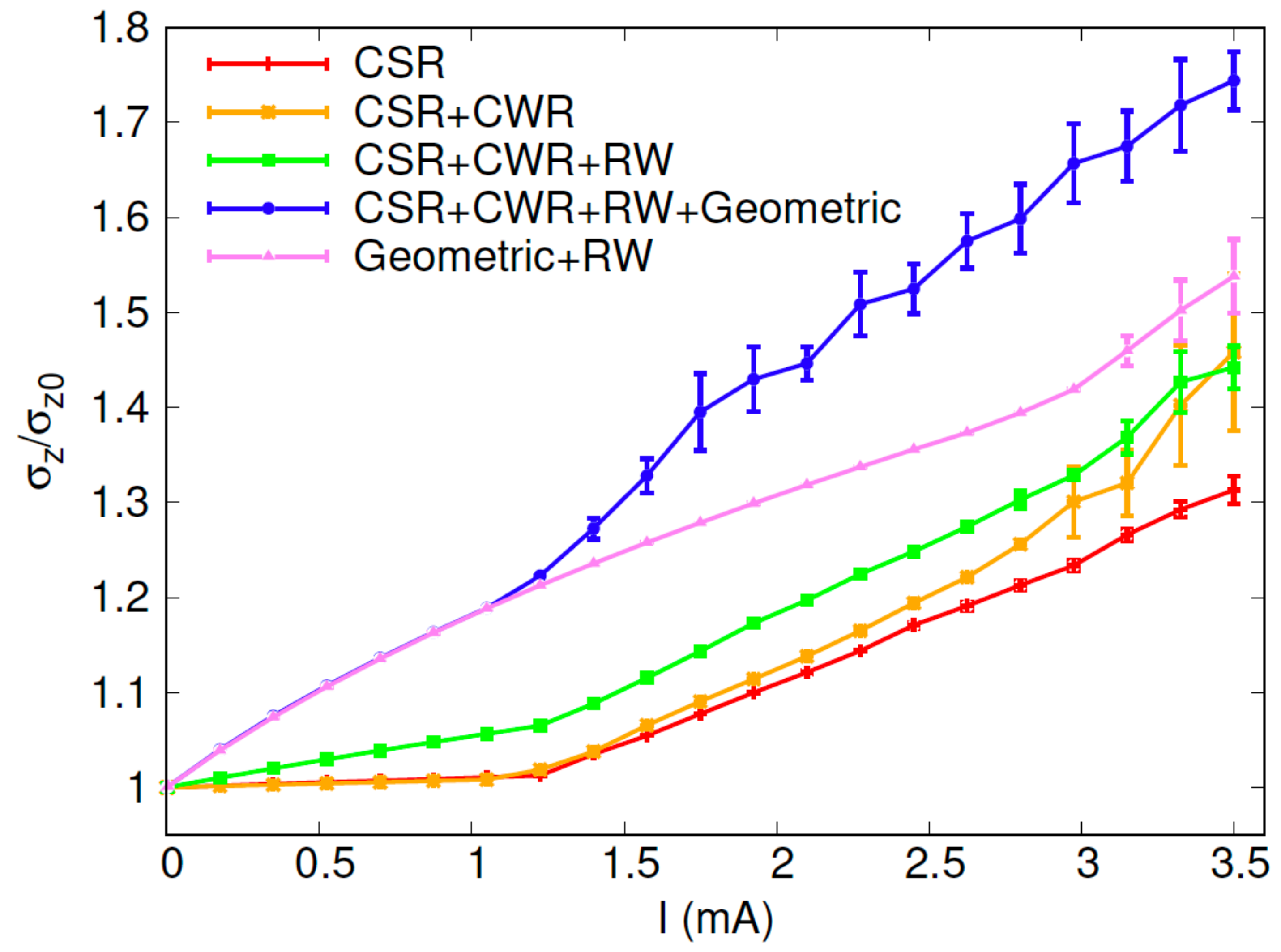

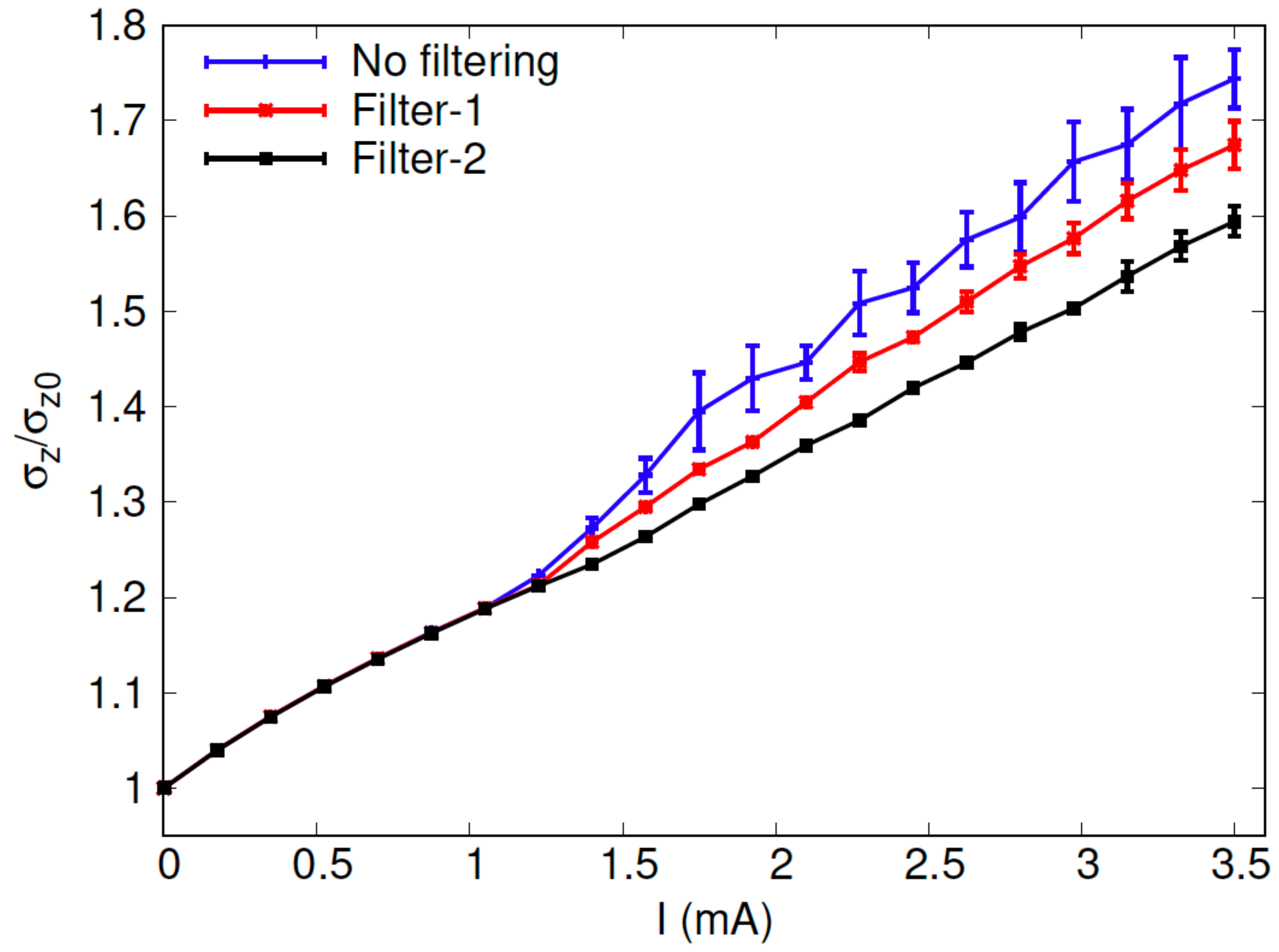

$\sigma_{z0} = 4.6$ mm

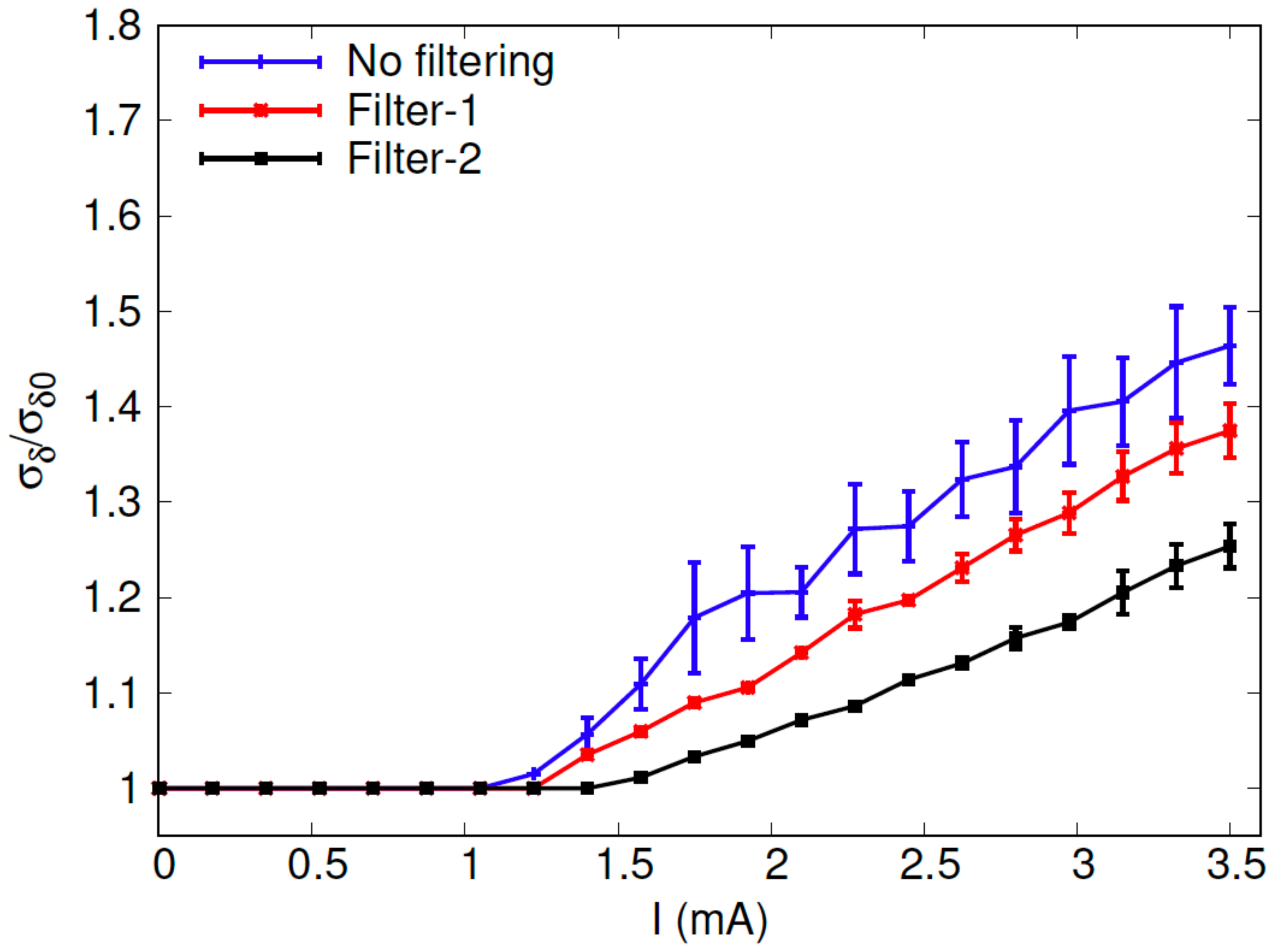

$\sigma_{\delta 0} = 7.53 \times 10^{-4}$

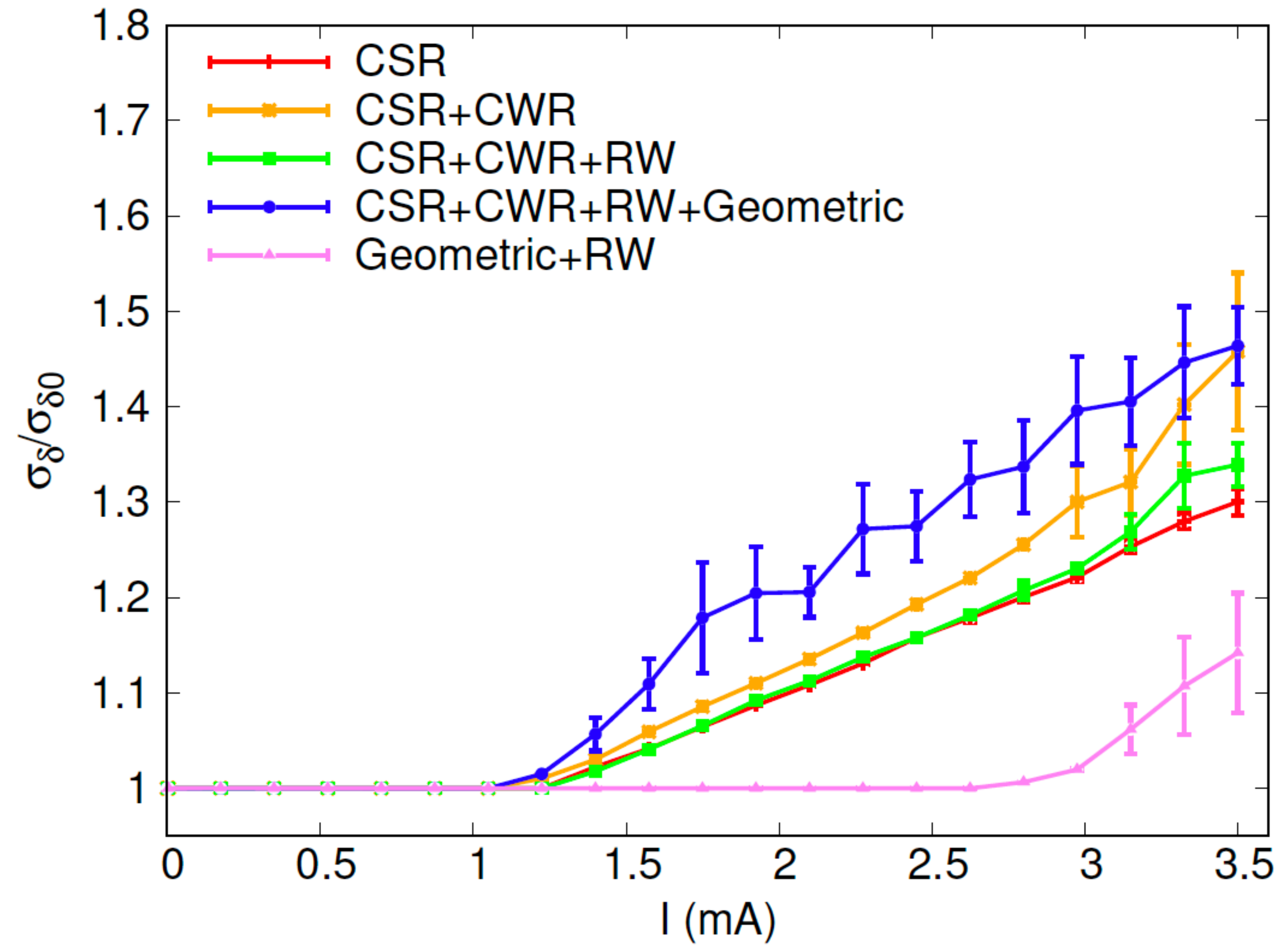

Prediction of CSR instability via simulations (cont'd)

- Example-2: Elettra 2.0 (in collaboration with S. Dastan)
  - Step-1: Impedance modeling of CSR by CSRZ, RW by IW2D, and geometric wakes by broadband resonator (BBR).
    - Alternative CSR models: CSRZ, PP, filtered PP
    - $h = 7.5$ mm, $\bar{\rho} = 7.8$ m
    - BBR: Q=1, f_r=7 GHz, $R_s \approx 3000\ \Omega$ ($|\mathrm{Im}[Z_{\|}]/n| = 0.5\ \Omega$ [1])

Elettra, Sincrorone Trieste, Italy
Courtesy of E. Karantzous

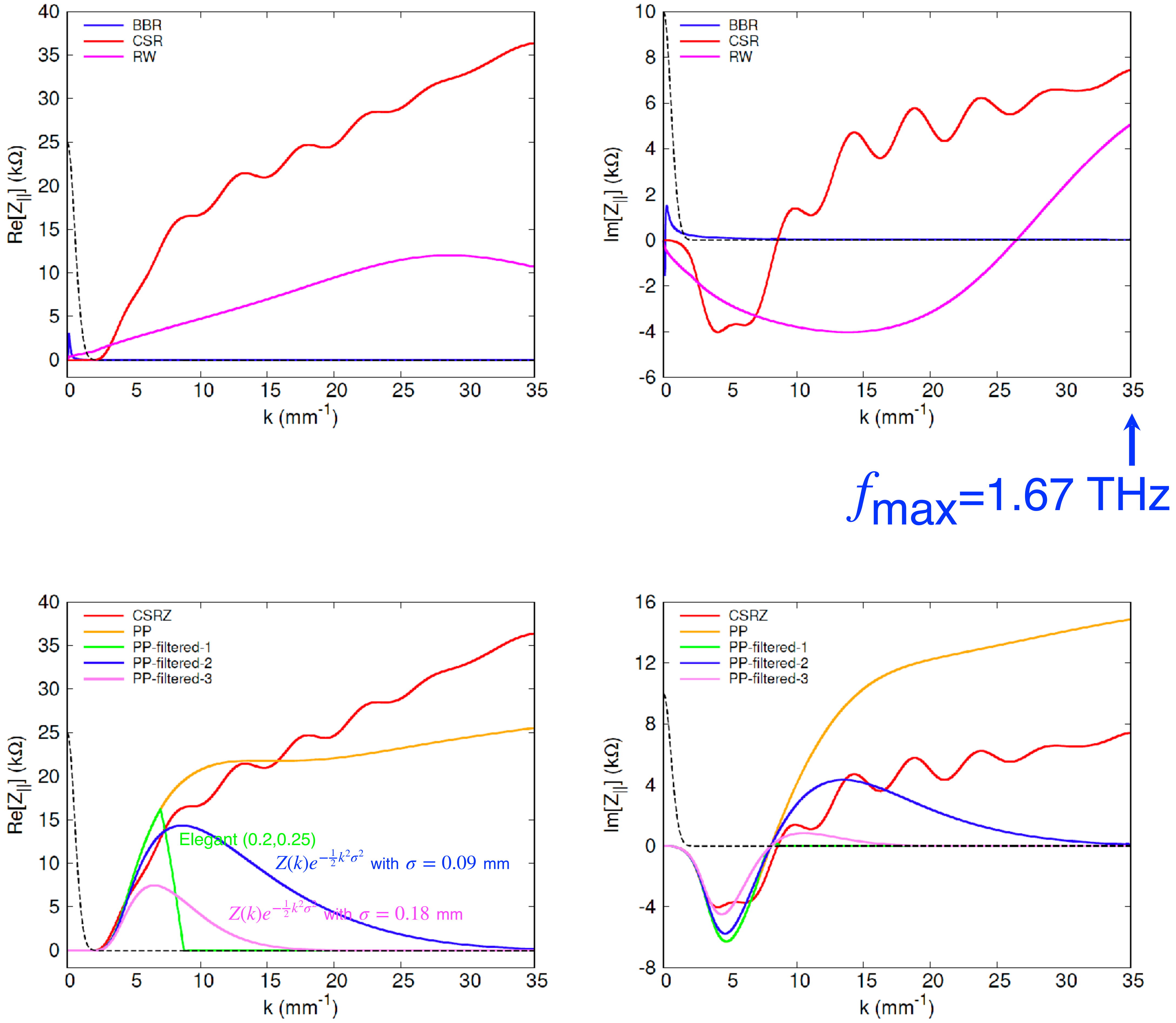

[1] Elettra 2.0 TDR, Part three: Machine and Infrastructure.

Prediction of CSR instability via simulations (cont'd)

- Example-2: Elettra 2.0 (in collaboration with S. Dastan)
  - Step-2: Instability analysis to determine $I_{\text{th}}(k)$.
    - σ_{z0}=1.8 mm without harmonic cavity (3HC)
  - Step-3: Choosing important parameters: maximum k_{max} for impedance model, minimum mesh size $\Delta z \ll 2\pi/k_{\text{max}}$.
    - k_{max}=35 mm^{-1} $\rightarrow$ f_{max}=1.67 THz.

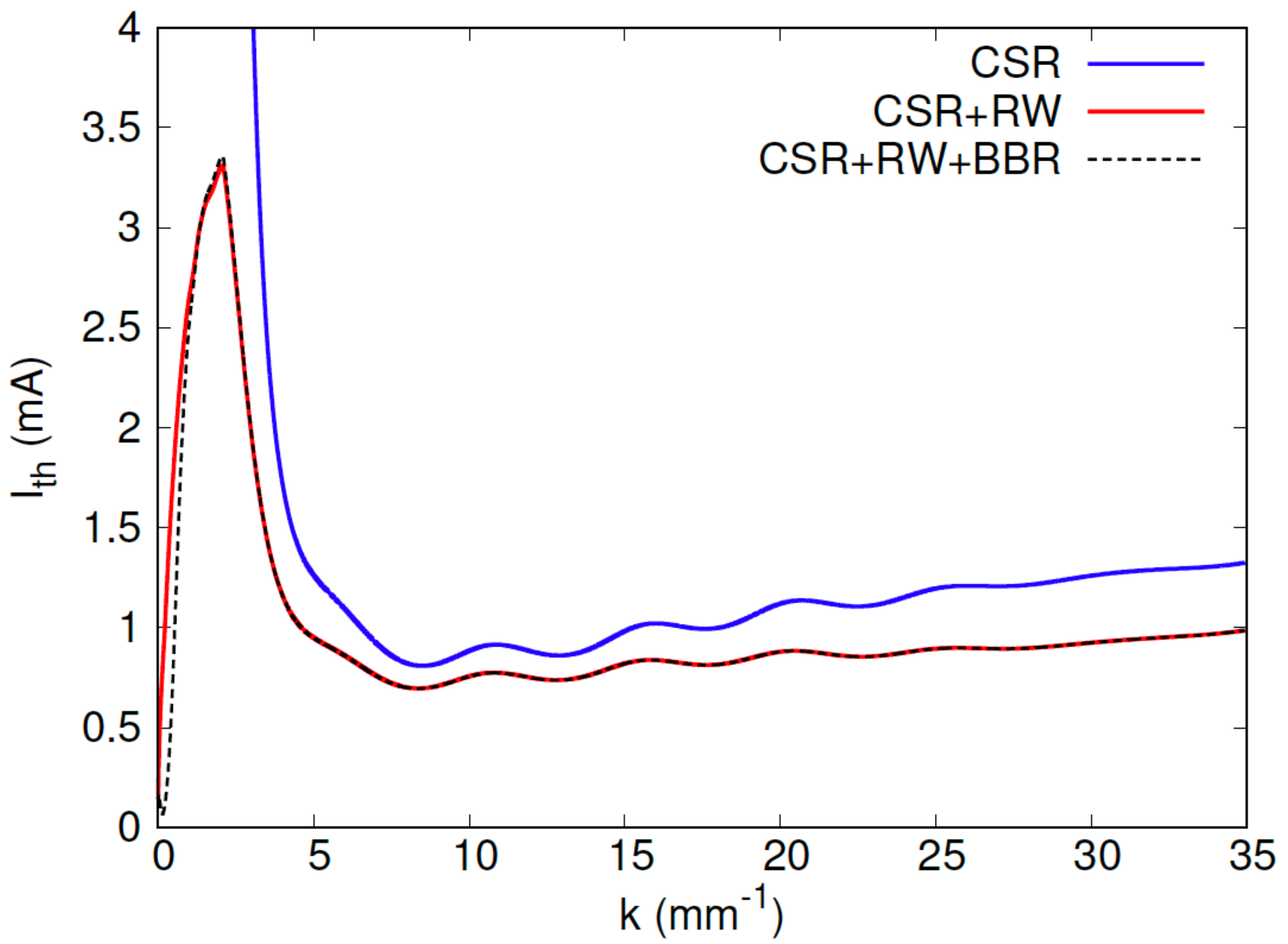

CSR and RW re important source for MWI in Elettra 2.0

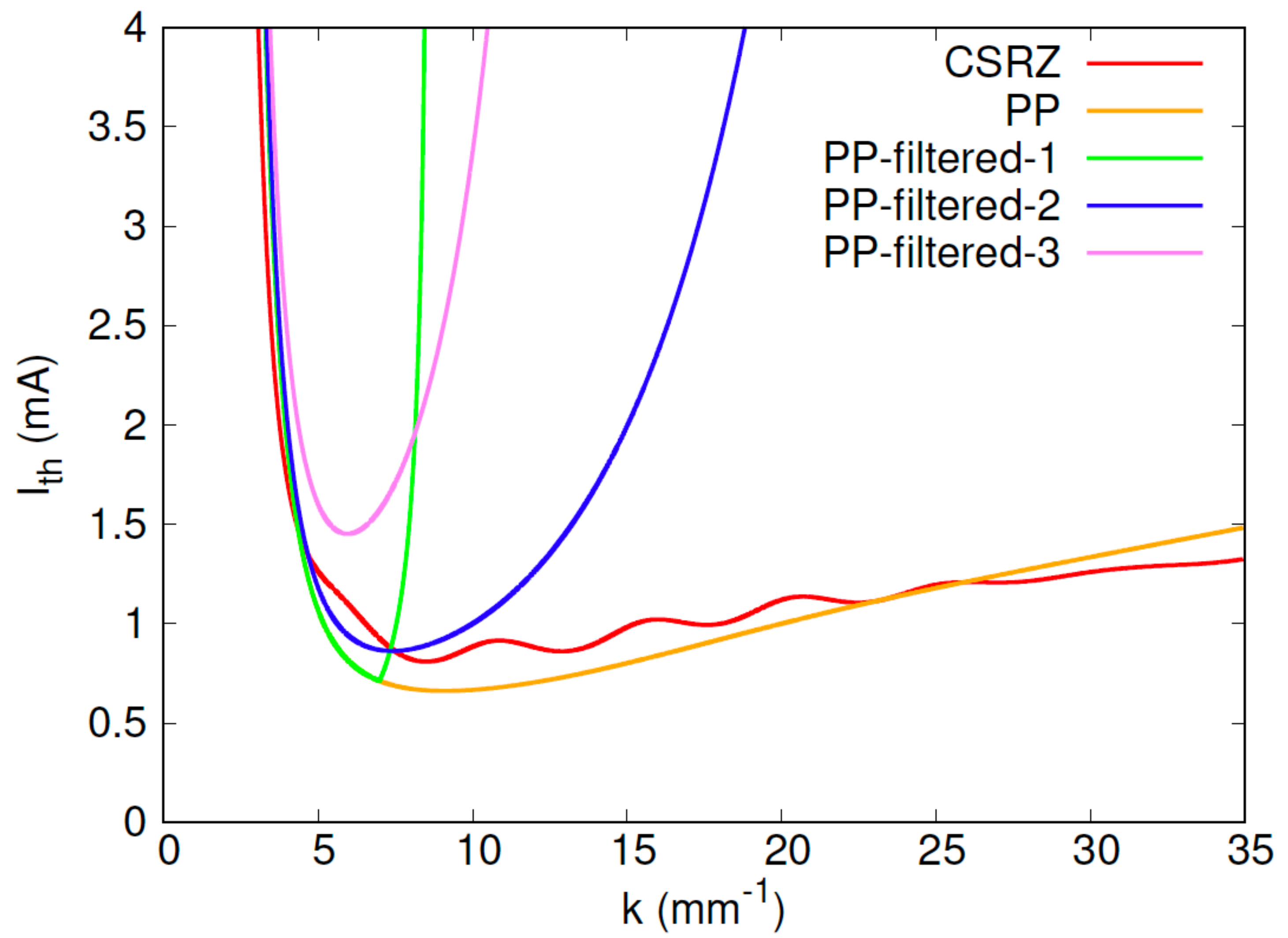

Filtered impedance models predicts higher MWI threshold

Elettra 2.0 parameters

Paremeter	Elettra 2.0		Unit
	without 3HC	With 3HC	-
Energy (E)	2.4		GeV
Circumference (C)	259.2		m
Bunch length (σ_z)	1.8	4.5	mm
Synchrotron Tune (Q_s)	2.6e-3		-
Energy spread (σ_p)	0.091e-2		-
Longitudinal damping time (τ_δ)	0.0067		s
Compaction factor (α_c)	1.2e-4		-
Bending radius (ρ)	Type1: 10.19 Type 2: 7.05 Type 3(anti-bend): 34.37 average(type1&2)=7.81		m
Bending length (L)	Type 1: 0.64 Type 2: 0.80 Type 3 (anti-bend): 0.24		m
Vacuum chamber size (h)	7.5e-3		m
Critical wave number (k_c)	1.99e+10		m^{-1}
Wall shielding threshold (k_w)	4.78e+3		m^{-1}
Radiation formation length (l_f)	1.39	1.87	m
Catch-up distance (l_c)	0.42		m
Slippage length (l_s)	2.83e-5		m
Π	7.48	19.37	-
Π_{RW}	34.40	96.01	-
I_{th1}	0.7	1.9	mA
I_{th2}	0.73	1.8	mA
I_{th3}	2.4	6.1	mA

Prediction of CSR instability via simulations (cont'd)

- Example-2: Elettra 2.0 (in collaboration with S. Dastan)
  - Step-4: Run tracking simulations (Elegant) and VFP simulations (Only consider CSR)
    - General consistency between theory, Elegant and VFP simulations.
    - 3HC increases MWI threshold through reducing charge density as expected.

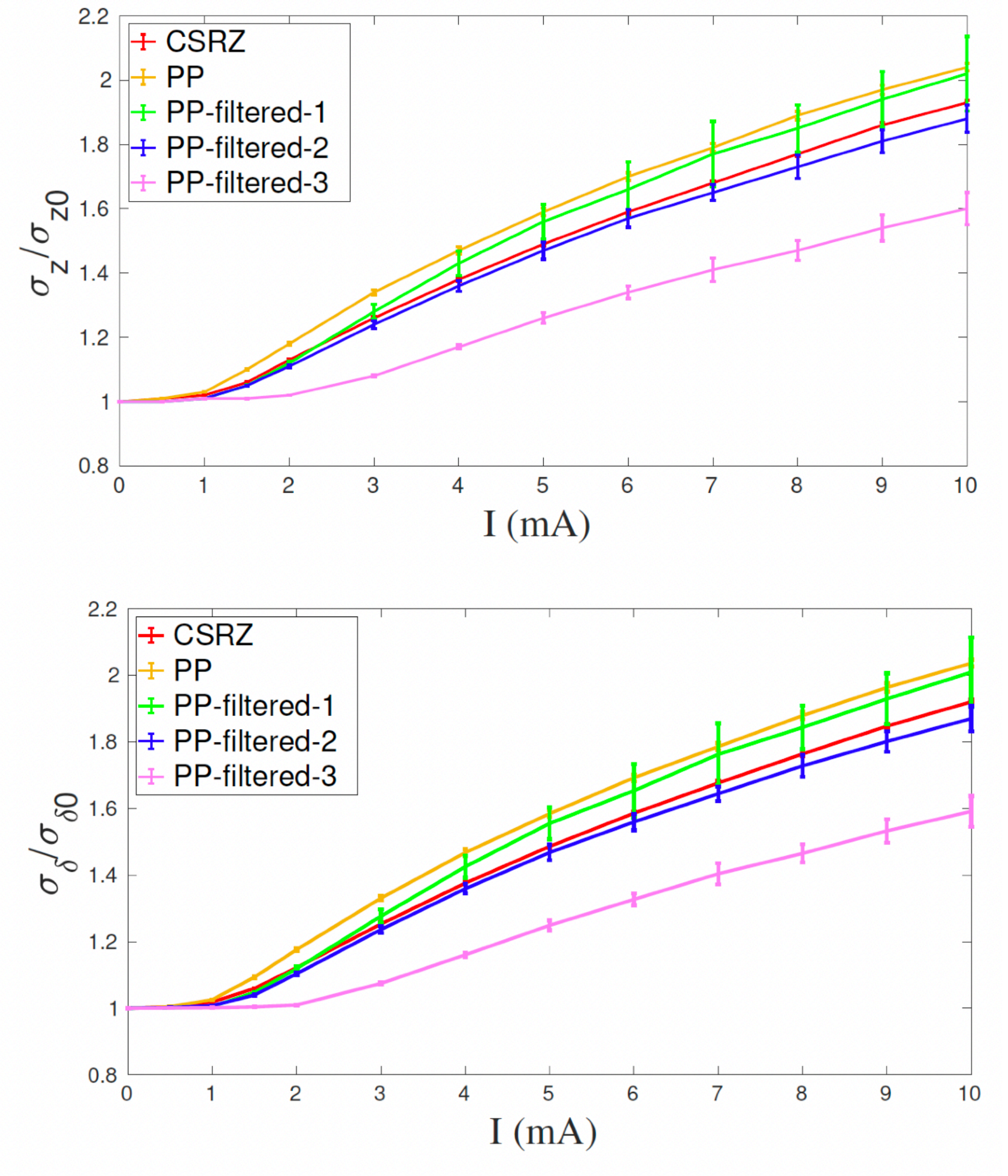

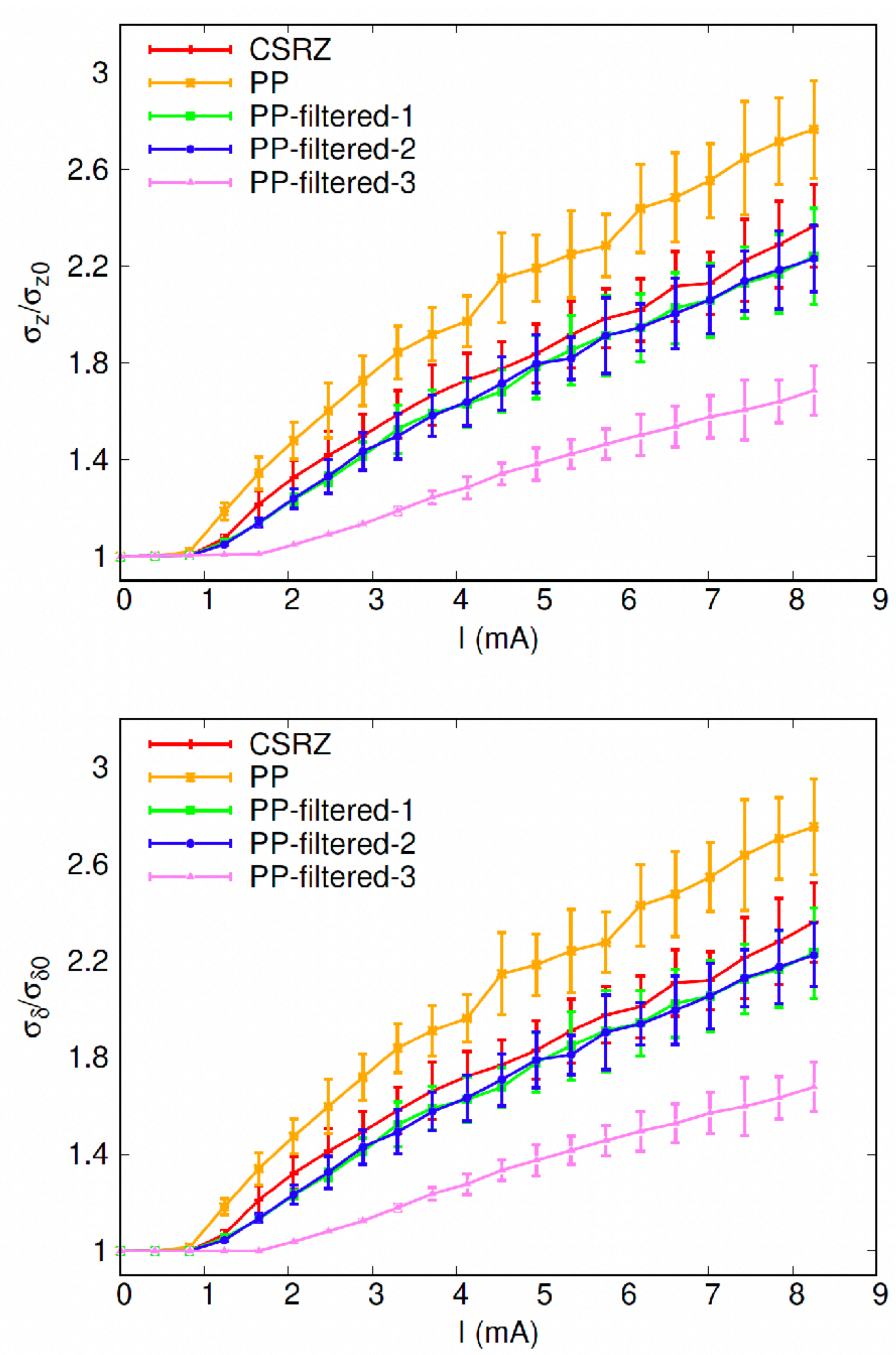

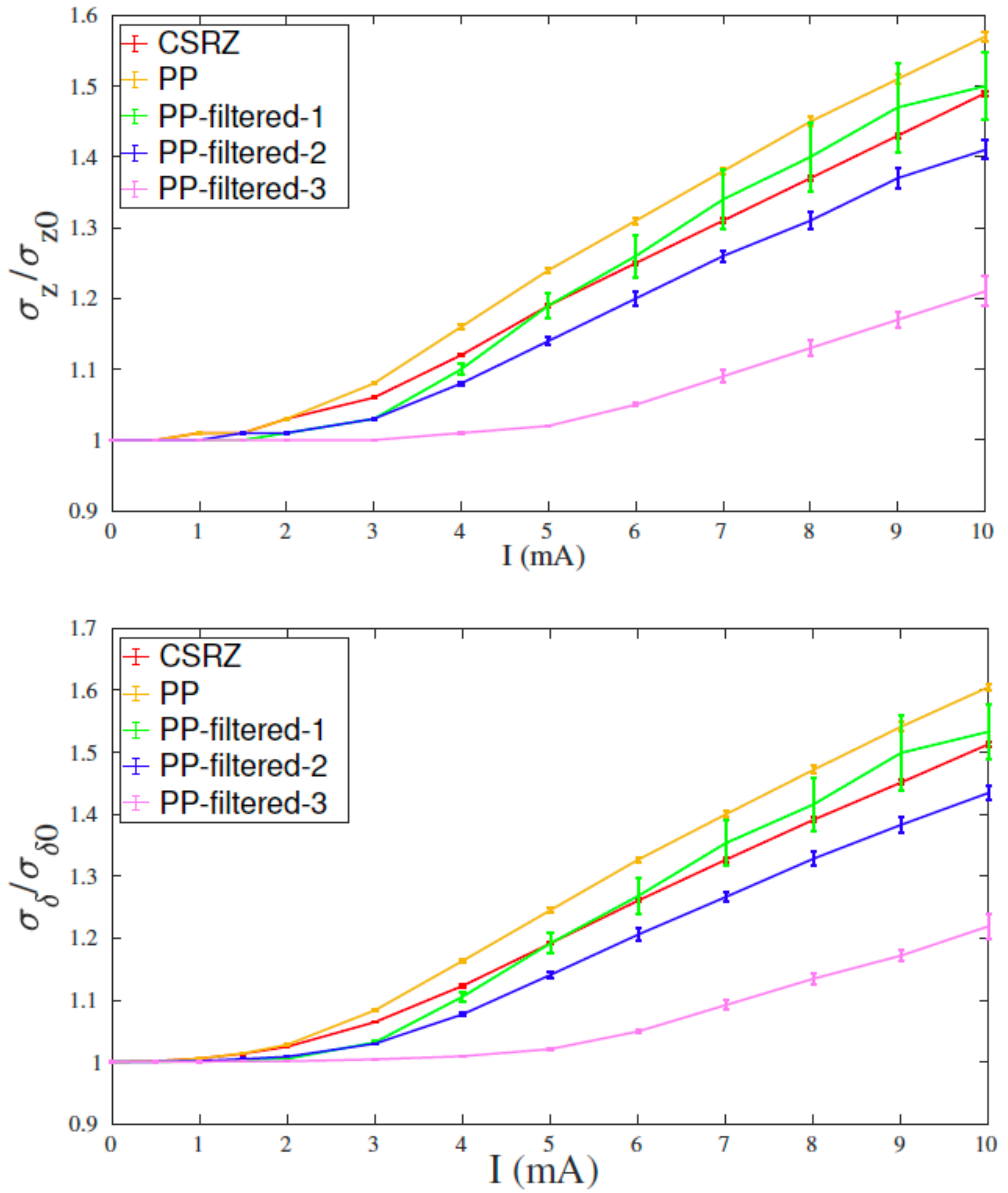

Prediction of CSR instability via simulations (cont'd)

- Example-2: Elettra 2.0 (in collaboration with S. Dastan)
  - Step-4: Run tracking simulations (Elegant) simulations (Interplay of CSR, RW and BBR)
    - The (preliminary) results with 3HC seems to suggest that CSR is not a threat at Elettra 2.0.
  - Step-5: Check consistency between theories and simulations.
    - The results with BBR seems plausible. Further investigations (detailed calculations of geometric impedances and benchmarks with VFP solver) are planned. Realistic geometric impedance model is preferred.

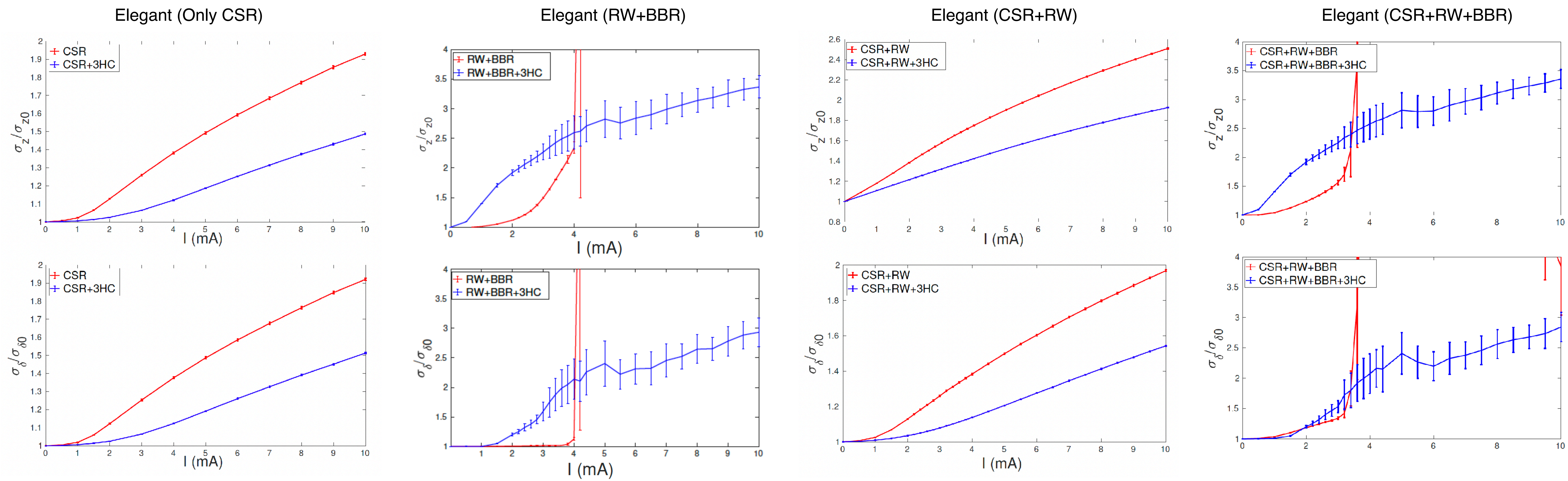

Comment from R. Lindberg (ANL): Elegant has difficulty when $k_r\sigma_z \lesssim 1$ (k_r: resonant frequency of BBR). Also true for VFP solver.

Summary

- CSR is a hot topic of accelerator physics.
- Analytic theories (S-H theory and its extensions) are useful for determining the significance of CSR in low-emittance electron storage rings.
- Calculated high-frequency ($k\sigma_z \gg 1$) impedances (CSR, RW, and geometric impedances which might be overlooked in impedance modelings) can be used to estimate MWI threshold.
- Care should be taken in simulations of MWI with high-frequency ($k\sigma_z \gg 1$) impedances.
  - Play with “numerical arts”.

- Not covered in this talk:
  - Narrow-band CSR impedance and its impact on MWI [1]
  - Accurate prediction of beam dynamics in the region well above MWI threshold

- Looking for collaborations on CSR, CWR/CUR, space charge (SC) and resistive wall (RW)
  - CSR/CWR/SC/RW field dynamics: Theories and simulations
  - CSR/CWR/SC/RW effects in linacs and storage rings: Theories and simulations

[1] Y. Cai, Phys. Rev. ST Accel. Beams **17**, 020702 (2014).

Backup

Analytic theories of CSR driven MWI threshold (cont'd)

- Apply S-H theory to electron storage rings
  - Quick estimate of CSR instability.
  - Very useful in the design stage of a storage ring.
  - "Yellow region" indicates "severity of instability".
  - For rings where CSR is marginally of concern, MWI simulations are required.

Parameters	SuperKEKB DR[1]	SLC DR[2]	ATF[3]	SuperKEKB LER[4]	SuperKEKB LER[5]	PEP-II LER[6]	ALS[6]	KEKB LER[7]
Circumference (m)	135.5	35.27	138.6	3016	3016	2200	196	3016
Energy (GeV)	1	1.21	1.54	4	3.5	3.1	1.5	3.5
Bending radius	2.43623	2.0372	5.73	15.87	15.87	13.7	4	15.87
Mom. compaction	3.43E-03	0.01814	2.17E-03	2.74E-04	2.74E-04	1.31E-03	1.41E-03	3.31E-04
Energy spread(10^{-4})	5.44	7.3	5.56	8.14	7.13	8.1	7.1	7.27
Bunch length (mm)	5.1	5.9	5	6	3	10	7	4.58
Bunch population (10^{10})	5	5	2	9.03	11.7	9.16	12.3	6.47
Pipe height@bends (mm)	34	15.6	24	90	90	50	40	94
Total bend. radius(2π)[8]	1	1	1	1	1	1	1	1

1) Design Version 1.140, Apr. 2010
2) SLC design handbook, Dec. 1984
3) ATF design and study report, KEK Internal 95-4
4) Nano-beam option design, Feb. 2008
5) High-current option design
6) G. Stupakov and S. Heifets, PRST-AB 5, 054402 (2002)
7) Machine operating parameters, Jun.17, 2009
8) Assumed

SuperKEKB DR (Design Ver. 1.140)

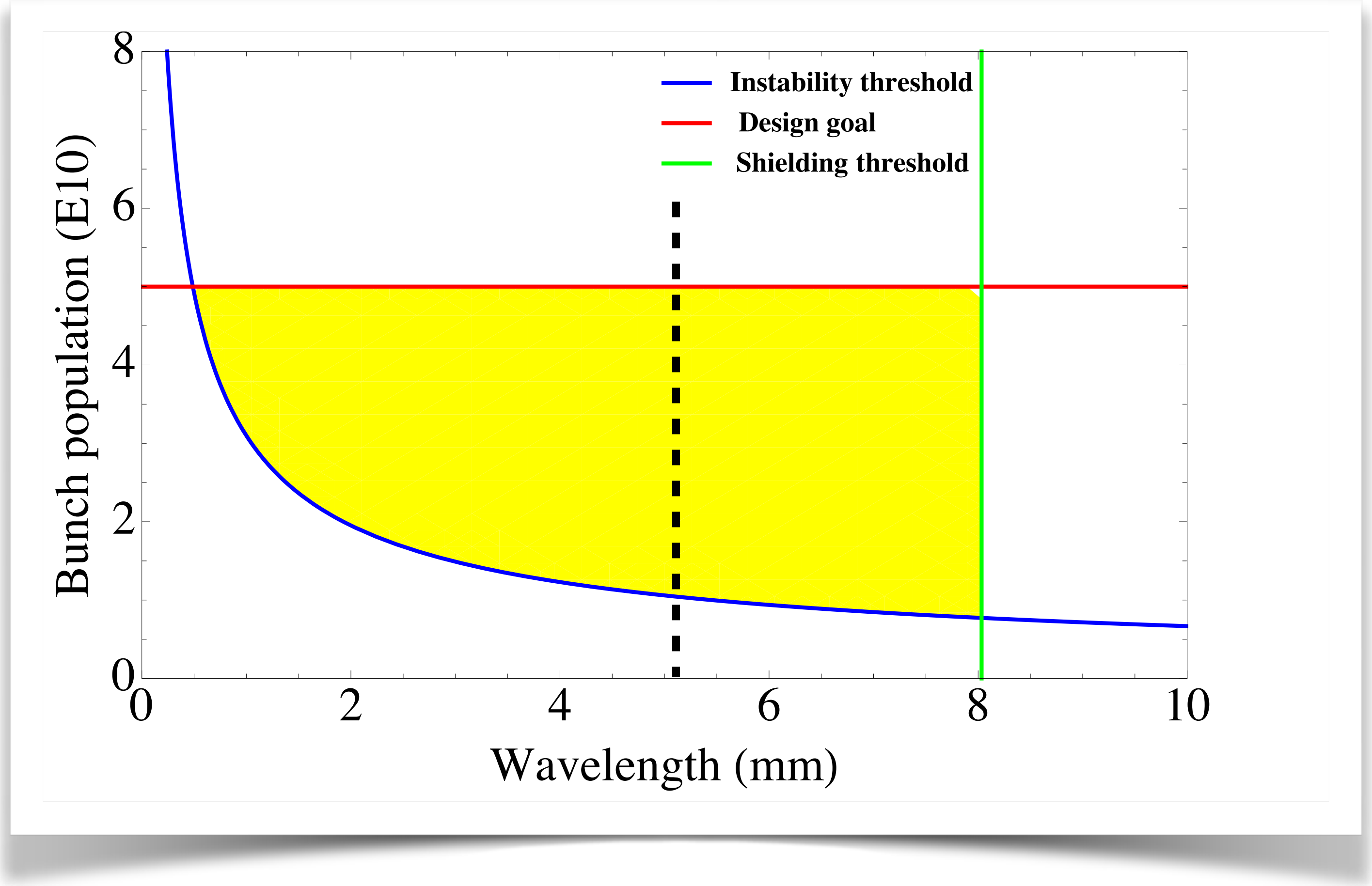

SuperKEKB LER (Design nano-beam option)